UNIVERSITY OF MINNESOTA
ST. ANTHONY FALLS LABORATORY
Engineering, Environmental and Geophysical Fluid Dynamics

PROJECT REPORT 468

Physical Model Study of the Intake Structure of the Prairie Du Sac Hydroelectric Project

By

Omid Mohseni, Matthew Lueker, Richard Christopher and Heinz Stefan

Prepared for
Mead&Hunt and Wisconsin Power and Light Company

March 2006
Minneapolis, Minnesota

The University of Minnesota is committed to the policy that all persons shall have equal access to its programs, facilities, and employment without regard to race, religion, color, sex, national origin, handicap, age or veteran status.

Abstract

A physical model study of the intake structure of the Prairie du Sac Hydroelectric Project was conducted to assess the distribution of velocities across the intake as an aid in identifying possible modifications to meet resource agency fish protection criteria. The model was built at a scale of 1 to 14.

In the model study, approach velocity characteristics were evaluated for a new trash rack placed upstream of the intake structure replacing the existing trash rack inside the structure. Two modification scenarios were studied: a trash rack with 1.75-inch openings (68% opening ratio), and a trash rack with 1.0-inch openings (53% opening ratio).

Flow velocities were measured at 40 locations upstream of the model trash rack, corresponding to points located approximately one foot upstream of the trash rack in the full-scale (prototype) structure. Flow velocity measurements were conducted under three flow conditions: 1300 cfs (representing typical flow through the project's 3 larger generating units) 1000 cfs (representing typical flow through the project's 5 smaller generating units), and 2170 cfs (representing maximum flow possible through the project's largest generating unit). Under the 1300 cfs flow condition, the approach flow velocities did not exceed 1.1 and 1.2 fps with the 1.75- and 1.0-inch opening trash racks, respectively. The maximum through flow velocities for the 1300 cfs flow condition were estimated to be 1.9 and 2.4 fps, respectively.

Acknowledgements

The work reported herein was supported by Mead & Hunt and Wisconsin Power & Light Company (WP&L). We would like to thank James Tucker and Benjamin Erickson of St. Anthony Falls Laboratory for their contribution to the model construction and instrumentation.

Table of Contents

Abstract ii

Acknowledgements iii

List of Figures v

List of Tables ix

1. Introduction 1

2. Model Construction 4

2.1. General Features of the Physical Model 4

2.2. Instrumentation 5

2.3. Model Modifications 6

3. Model Runs and Results 14

3.1. Modeling of Trash Rack 14

3.2. Trash Rack with 1.75-inch Openings 15

3.3. Trash Rack with 1.0-inch Openings 20

4. Summary 25

References 26

Appendix A: Longitudinal Profiles of the River Bed Upstream of the Intake 27

Appendix B: Repeatability Test 31

Appendix C: New Test Series with Trash Racks at the Existing Location 32

C.1. Test Series # 1: Existing Ice-Wall and Trash Rack with 1.75-inch Openings 34

C.2. Test Series # 2: Existing Ice-Wall and Trash Rack with 1.0-inch Openings 41

C.3. Test Series # 3: Ice-Wall with 3-ft Submergence and Trash Rack with 1.75-inch Openings 48

C.4. Test Series # 4: Ice-Wall with 3-ft Submergence and Trash Rack with 1.0-inch Openings 57

Appendix D: Intermediate Test Series 67

List of Figures

Figure 1. Location of the Prairie du Sac Hydroelectric Project. 1
Figure 2. General layout of the Prairie du Sac Hydroelectric Project: the dam, navigation lock and the power house. 2
Figure 3. The Prairie du Sac power house. The red line shows the outline of the section used for the physical model study. 2
Figure 4. A cross-section of a single unit of the Prairie du Sac power house. The red line shows the outline of the section used for the physical model study. 3
Figure 5. Plan and cross-section of the model constructed in St. Anthony Falls Laboratory. ... 7
Figure 6. Model runners. 8
Figure 7. The 6-inch gate valves on the draft tubes. 8
Figure 8. The model was built of plywood and lumber. 9
Figure 9. The three-dimensional Acoustic Doppler Velocimeter (ADV) to measure approach velocity approximately one inch upstream of the trash rack. 9
Figure 10. A longitudinal cross-section of the model after modifying the head tank and raising the bed elevation by 4 11/16 inches (5.5 feet for the prototype). 10
Figure 11. View of the modified head box, looking downstream. 11
Figure 12. To dissipate the large eddies formed in the head box, wire mesh and two honeycomb screens were installed downstream of the rock crib. 11
Figure 13. The elbow meter consisting of a Meriam manometer and two pressure taps on the 12-inch water supply line was used to measure the total flow rate 12
Figure 14. The elbow meter rating curve. 13
Figure 15. The x-component of the velocity measured at 40 locations, 1.2 ft away from a trash rack with 1.75-inch openings, under the 1300 cfs flow condition. The actual measured flow was 1305 cfs. Vertical lines show the position of the piers. 17
Figure 16. The x-component of the velocity measured at 40 locations, 1.2 ft away from a trash rack with 1.75 inch openings, under the 1000 cfs flow condition. The actual measured flow was 940 cfs. Vertical lines show the position of the piers. 18
Figure 17. The x-component of the velocity measured at 40 locations, 1.2 ft away from a trash rack with 1.75-inch openings under the 2170 cfs flow condition. The actual measured flow was 2193 cfs. Vertical lines show the position of the piers. 19
Figure 18. The x-component of the velocity measured at 40 locations, 1.2 ft away from a trash rack with 1.0-inch openings, under the 1300 cfs flow condition. The actual measured flow was 1335 cfs. Vertical lines show the position of the piers. 22
Figure 19. The x-component of the velocity measured at 40 locations, 1.2 ft away from a trash rack with 1.0-inch openings, under the 1000 cfs flow condition. The actual measured flow was 985 cfs. Vertical lines show the position of the piers. 23
Figure 20. The x-component of the velocity measured at 40 locations, 1.2 ft away from a trash rack with 1.0-inch openings, under the 2170 cfs flow condition. The actual measured flow was 2200 cfs. Vertical lines show the position of the piers. 24
Figure B.1. The x-component of the velocity measured at 40 locations, 1.2 ft away from a trash rack with 1.0-inch openings, under the 2170 cfs flow condition. The actual measured flow was 2200 cfs. This was a repeatability test for the test shown in Figure 20. 31
Figure C.1. A longitudinal cross-section of the model after replacing one of the outside walls

with Plexiglas and placing the trash rack in its exiting location. 33
Figure C.2. The x-component of the velocity measured at 30 locations inside the bay areas, 2.9 ft away from a trash rack with 1.75-inch openings at its current location, under the 1000 cfs flow condition. The actual measured flow was 981 cfs. 35
Figure C.3. The z-component of the velocity measured at 30 locations inside the bay areas, 2.9 ft away from a trash rack with 1.75-inch openings at its current location, under the 1000 cfs flow condition. The actual measured flow was 981 cfs. 36
Figure C.4. The x-component of the velocity measured at 30 locations inside the bay areas, 2.9 ft away from a trash rack with 1.75-inch openings at its current location, under the 1300 cfs flow condition. The actual measured flow was 1258 cfs. 37
Figure C.5. The z-component of the velocity measured at 30 locations inside the bay areas, 2.9 ft away from a trash rack with 1.75-inch openings at its current location, under the 1300 cfs flow condition. The actual measured flow was 1258 cfs. 38
Figure C.6. The x-component of the velocity measured at 30 locations inside the bay areas, 2.9 ft away from a trash rack with 1.75-inch openings at its current location, under the 2200 cfs flow condition. The actual measured flow was 2150 cfs. 39
Figure C.7. The z-component of the velocity measured at 30 locations inside the bay areas, 2.9 ft away from a trash rack with 1.75-inch openings at its current location, under the 2200 cfs flow condition. The actual measured flow was 2150 cfs. 40
Figure C.8. The x-component of the velocity measured at 30 locations inside the bay areas, 2.9 ft away from a trash rack with 1.0-inch openings at its current location, under the 1000 cfs flow condition. The actual measured flow was 1012 cfs. 42
Figure C.9. The z-component of the velocity measured at 30 locations inside the bay areas, 2.9 ft away from a trash rack with 1.0-inch openings at its current location, under the 1000 cfs flow condition. The actual measured flow was 1012 cfs. 43
Figure C.10. The x-component of the velocity measured at 30 locations inside the bay areas, 2.9 ft away from a trash rack with 1.0-inch openings at its current location, under the 1300 cfs flow condition. The actual measured flow was 1258 cfs. 44
Figure C.11. The z-component of the velocity measured at 30 locations inside the bay areas, 2.9 ft away from a trash rack with 1.0-inch openings at its current location, under the 1300 cfs flow condition. The actual measured flow was 1258 cfs. 45
Figure C.12. The x-component of the velocity measured at 30 locations inside the bay areas, 2.9 ft away from a trash rack with 1.0-inch openings at its current location, under the 2200 cfs flow condition. The actual measured flow was 2150 cfs. 46
Figure C.13. The z-component of the velocity measured at 30 locations inside the bay areas, 2.9 ft away from a trash rack with 1.0-inch openings at its current location, under the 2200 cfs flow condition. The actual measured flow was 2150 cfs. 47
Figure C.14. The x-component of the velocity measured at 30 locations inside the bay areas, 2.9 ft away from a trash rack with 1.75-inch openings at its current location, under the 1000 cfs flow condition. The actual measured flow was 1012 cfs. The ice-wall was submerged 3-ft under normal water level conditions. 49
Figure C.15. The z-component of the velocity measured at 30 locations inside the bay areas, 2.9 ft away from a trash rack with 1.75-inch openings at its current location, under the 1000 cfs flow condition. The actual measured flow was 1012 cfs. The ice-wall was submerged 3-ft under normal water level conditions. 50
Figure C.16. The x-component of the velocity measured at 30 locations inside the bay areas,

2.9 ft away from a trash rack with 1.75-inch openings at its current location, under the 1300 cfs flow condition. The actual measured flow was 1305 cfs. The ice-wall was submerged 3-ft under normal water level conditions. 51
Figure C.17. The z-component of the velocity measured at 30 locations inside the bay areas, 2.9 ft away from a trash rack with 1.75-inch openings at its current location, under the 1300 cfs flow condition. The actual measured flow was 1305 cfs. The ice-wall was submerged 3-ft under normal water level conditions. 52
Figure C.18. The x-component of the velocity measured at 30 locations inside the bay areas, 2.9 ft away from a trash rack with 1.75-inch openings at its current location, under the 1600 cfs flow condition. The actual measured flow was 1608 cfs. The ice-wall was submerged 3-ft under normal water level conditions. 53
Figure C.19. The z-component of the velocity measured at 30 locations inside the bay areas, 2.9 ft away from a trash rack with 1.75-inch openings at its current location, under the 1600 cfs flow condition. The actual measured flow was 1608 cfs. The ice-wall was submerged 3-ft under normal water level conditions. 54
Figure C.20. The x-component of the velocity measured at 30 locations inside the bay areas, 2.9 ft away from a trash rack with 1.75-inch openings at its current location, under the 2200 cfs flow condition. The actual measured flow was 2164 cfs. The ice-wall was submerged 3-ft under normal water level conditions. 55
Figure C.21. The z-component of the velocity measured at 30 locations inside the bay areas, 2.9 ft away from a trash rack with 1.75-inch openings at its current location, under the 2200 cfs flow condition. The actual measured flow was 2164 cfs. The ice-wall was submerged 3-ft under normal water level conditions. 56
Figure C.22. The x-component of the velocity measured at 30 locations inside the bay areas, 2.9 ft away from a trash rack with 1.0-inch openings at its current location, under the 1000 cfs flow condition. The actual measured flow was 1012 cfs. The ice-wall was submerged 3-ft under normal water level conditions. 59
Figure C.23. The z-component of the velocity measured at 30 locations inside the bay areas, 2.9 ft away from a trash rack with 1.0-inch openings at its current location, under the 1000 cfs flow condition. The actual measured flow was 1012 cfs. The ice-wall was submerged 3-ft under normal water level conditions. 60
Figure C.24. The x-component of the velocity measured at 30 locations inside the bay areas, 2.9 ft away from a trash rack with 1.0-inch openings at its current location, under the 1300 cfs flow condition. The actual measured flow was 1282 cfs. The ice-wall was submerged 3-ft under normal water level conditions. 61
Figure C.25. The z-component of the velocity measured at 30 locations inside the bay areas, 2.9 ft away from a trash rack with 1.0-inch openings at its current location, under the 1300 cfs flow condition. The actual measured flow was 1282 cfs. The ice-wall was submerged 3-ft under normal water level conditions. 62
Figure C.26. The x-component of the velocity measured at 30 locations inside the bay areas, 2.9 ft away from a trash rack with 1.0-inch openings at its current location, under the 1600 cfs flow condition. The actual measured flow was 1588 cfs. The ice-wall was submerged 3-ft under normal water level conditions. 63
Figure C.27. The z-component of the velocity measured at 30 locations inside the bay areas, 2.9 ft away from a trash rack with 1.0-inch openings at its current location, under the 1600 cfs flow condition. The actual measured flow was 1588 cfs. The ice-wall

was submerged 3-ft under normal water level conditions. 64
Figure C.28. The x-component of the velocity measured at 30 locations inside the bay areas, 2.9 ft away from a trash rack with 1.0-inch openings at its current location, under the 2200 cfs flow condition. The actual measured flow was 2156 cfs. The ice-wall was submerged 3-ft under normal water level conditions. 65
Figure C.29. The z-component of the velocity measured at 30 locations inside the bay areas, 2.9 ft away from a trash rack with 1.0-inch openings at its current location, under the 2200 cfs flow condition. The actual measured flow was 2156 cfs. The ice-wall was submerged 3-ft under normal water level conditions. 66

List of Tables

Table 1. Prototype and model parameter values of a trash rack with 1.75-inch openings, under 1300 cfs. 16
Table 2. Prototype and model parameter values of a trash rack with 1.0-inch openings, under 1300 cfs. 20
Table D.1. Summary of the velocity measurements at the elevation of the lower end of the modified ice-wall and 2.9 feet away from the trash rack 68

1. Introduction

Wisconsin Power and Light Company (WP&L) requested a model study of the intake structure of the Prairie du Sac hydroelectric project to explore the approach flow velocity profiles associated with a trash rack upstream of the existing intake. The trash rack configuration would replace the existing trash rack located inside the intake structure behind an existing ice wall with a rack placed upstream of the ice wall.

The hydroelectric power plant is on the Wisconsin River at Prairie du Sac (Figures 1 and 2). The intake structure comprises 8 units. Each unit has a three-bay inlet and is equipped with four runners mounted on a single shaft (Figure 3) discharging through two draft tubes (Figure 4).

The scope of this study was to build a physical model of a single unit of the existing intake structure, incorporating a modification consisting of placing a trash rack on the upstream side of the intake. The physical model incorporated two trash rack opening alternatives: (1) 1.75-inch clear opening and (2) 1.0-inch clear opening. The study included a series of velocity measurements taken upstream of the trash rack under three different flow conditions.

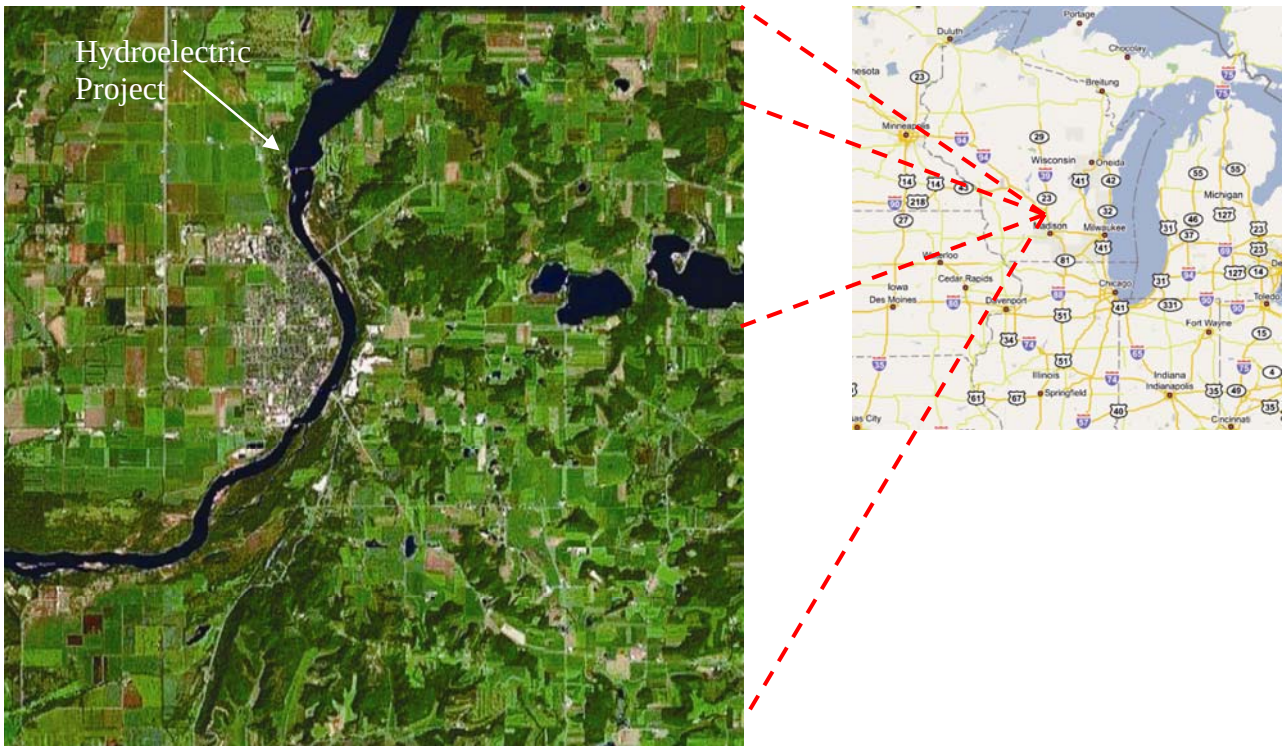

Figure 1. Location of the Prairie du Sac Hydroelectric Project.

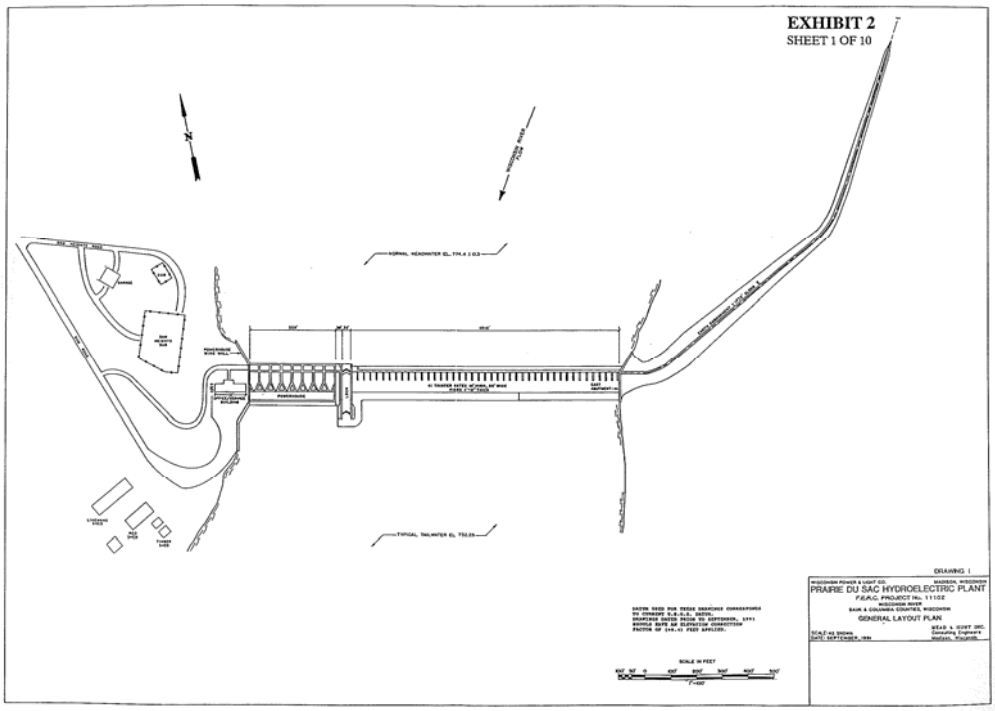

Figure 2. General layout of the Prairie du Sac Hydroelectric Project: the dam, navigation lock and the power house.

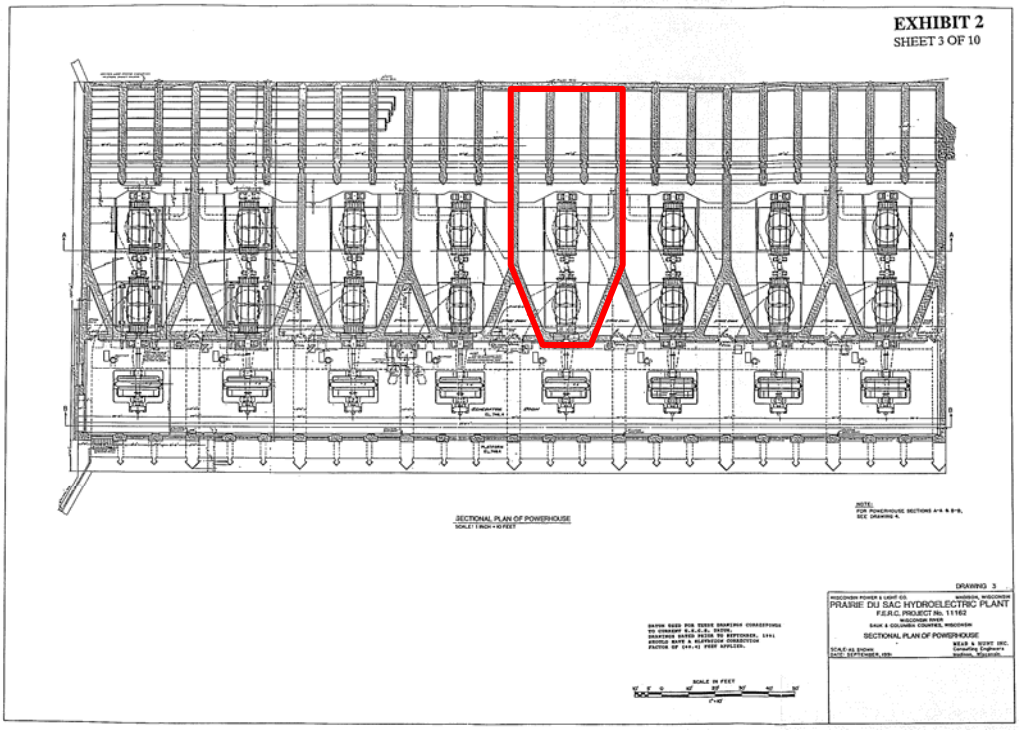

Figure 3. The Prairie du Sac power house. The red line shows the outline of the section used for the physical model study.

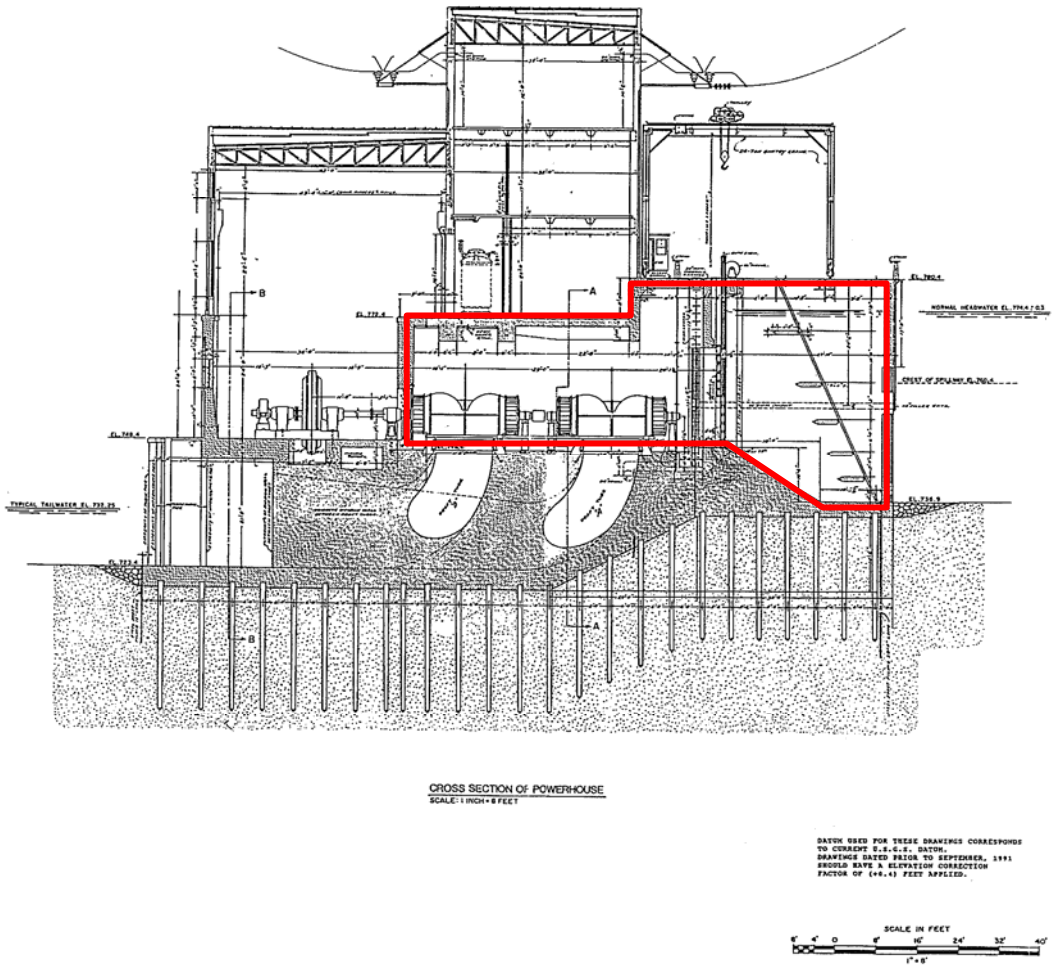

Figure 4. A cross-section of a single unit of the Prairie du Sac power house. The red line shows the outline of the section used for the physical model study.

2. Model Construction

The model was built at St. Anthony Falls Laboratory at a scale of 1:14. With flows scaled to Froude similarity, the flow patterns can be correctly reproduced in the model, while the flow regime stays turbulent. Using a 1:14 scale Froude similarity, flow parameters were scaled as follows:

Length	1:14
Area	1:196
Volume	1:2744
Flow rate	1:733.4
Velocity	1:3.74
Time	1:3.74

2.1. General Features of the Physical Model

Figure 5 shows the layout (plan view) and a longitudinal cross-section of the constructed model. The physical model consisted of a head tank upstream of the intake, an approach channel and a single unit of the power house. To simulate the approach flow of a single unit, the width of the approach channel was equal to the distance from the centerlines of the separating walls of a single unit.

In the model, Mississippi River water was discharged into the head tank using a multi-port diffuser. In the head tank, water, after being discharged through the ports of the diffuser, flowed over a weir into a stilling basin with a second overflow weir. The head tank was filled with rocks and screens to dissipate the energy of the upwelling flow near the crest of the weir. A short sill, wire mesh, a honeycomb screen, and a floating board were used to minimize the surface turbulence of the approaching flow and to create a quasi-uniform flow condition.

The model intake comprised three bays and a simulated turbine intake where the runners were located. The runners were simulated by building two parallel disks with diameters and clearances representative of the turbine runner, at the scale of 1:14 (Figure 6). Two model runners were attached to a single 6-inch tee-fitting. The 6-inch tee-fitting was connected to a 6-inch draft tube. Each draft tube was connected to a gate valve for adjusting the flow through each couple of runners (Figure 7). To accurately simulate water surface elevations upstream of

the intake, the 6-inch gate valves were partially closed until the upstream water surface elevation was maintained.

The model was built of plywood, sealed and painted to minimize leakage (Figure 8). The ceiling of the runner chamber was built from Plexiglas for visualization. Model features included an ice wall that is part of the original construction of the full-scale prototype. The ice wall in the model was built as an adjustable wall to accommodate the possible modeling of ice wall modifications. However, model test results indicated that moderate velocities occur in the vicinity of the ice wall, and modeling of alternative ice wall configurations was therefore not requested.

The water supply into the multi-port diffuser upstream of the head tank was controlled by a 10-inch butterfly valve on the water supply line connected to the Laboratory Supply Channel.

2.2. Instrumentation

To measure water surface elevation, three wet wells were provided. The wet wells were used to measure the water level upstream of the power house intake, to measure the flow rate through the runners, and to estimate the head loss through the trash rack. The wells were connected via ¼-inch plastic tubes to pressure taps in the floor/wall of the model. Water levels in the wet wells were measured using point gages with a precision of 0.001 ft. The zero points of all gages were determined from a single datum when the entire model was filled with standing water.

To measure water velocity, a carriage was built and installed on the model, which could travel upstream of the intake structure. A three-dimensional Sontek FlowTracker Acoustic Doppler Velocimeter (ADV) was mounted on the carriage, which could measure the velocity of a cylindrical sampling volume (0.24 inch diameter, 0.35 inch height) located 6 inches away from the probe with accuracy of +/- 1.0% (Figure 9). The ADV was tested on the diagnostic mode and showed that it could measure velocity one inch away from the model trash rack, i.e. 1.2 ft away from the prototype trash rack.

To measure total flow through the model, a pressure tap was mounted upstream of the sharp-crested weir in the head tank. The pressure tap was connected to a graduated wet well. The wet well readings were calibrated using the SAFL weigh tanks.

2.3. Model Modifications

During initial testing and velocity measurements, it became evident that the approach flow velocities downstream of the honeycomb screen were not uniformly distributed across the width. The non-uniform velocity distribution was due to large eddies formed downstream of the weir, which did not completely dissipate as water flowed through the wire mesh and the honeycomb screen. Therefore, it was decided to modify the head tank to prevent the production of large eddies. To accomplish this goal, the weir wall was removed and a rock crib was constructed, i.e. the head tank was filled with rocks with wire screens around them as shown in Figure 10. Downstream of the crib (Figure 11), another screen was provided to trap any debris from the Mississippi River water. In addition, two sets of honeycomb screens were installed to redistribute the flow and to ensure a quasi-uniform approach flow (Figure 12). This configuration was developed by trial and error until the flow velocities leaving the downstream honeycomb screen were relatively uniform to within ±10% across the width.

Subsequently, flow was measured on the water supply line using an elbow meter (Figure 13). The 12-inch elbow at the bottom of the vertical drop of the supply line was replaced with an elbow that was already equipped with elbow flow meter taps. The taps were located on the inner and outer curve of the elbow. A manometer filled with Red Meriam was connected to the pressure taps. The elbow flow meter showed immediate changes in readings when the flow varied in the pipe. Since the precision of the pressure reading on the manometer was one-tenth of an inch and the lowest flow rate caused a pressure difference of only 0.9 inches, the weigh tanks were used to verify the lowest flow rate. The rating curve of the elbow meter obtained by using the SAFL weigh tanks is given in Figure 14.

In addition to the modification to the head tank and flow measurement, Mead & Hunt provided new data regarding the bathymetry of the river upstream of the intake structure (see Appendix A). After consultation with the Mead & Hunt representatives, it was decided to modify the approach channel by raising the bed elevation by 5.5 feet. Figure 10 displays a longitudinal profile of the model with the modifications made to the head tank and the floor bed elevation.

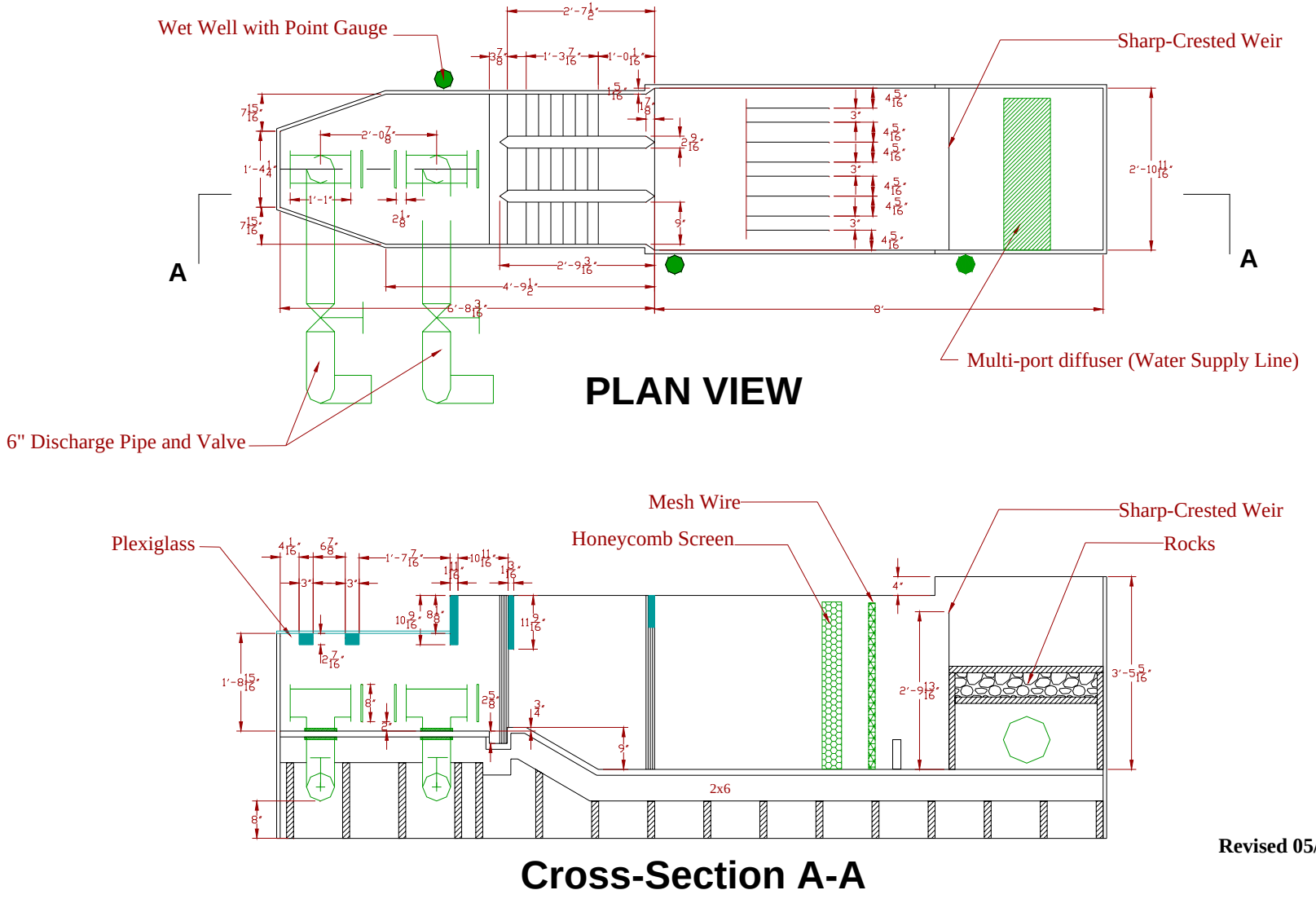

Figure 5. Plan and cross-section of the model constructed in St. Anthony Falls Laboratory.

Figure 6. Model runners.

Figure 7. The 6-inch gate valves on the draft tubes.

Figure 8. The model was built of plywood and lumber.

Figure 9. The three-dimensional Acoustic Doppler Velocimeter (ADV) to measure approach velocity approximately one inch upstream of the trash rack.

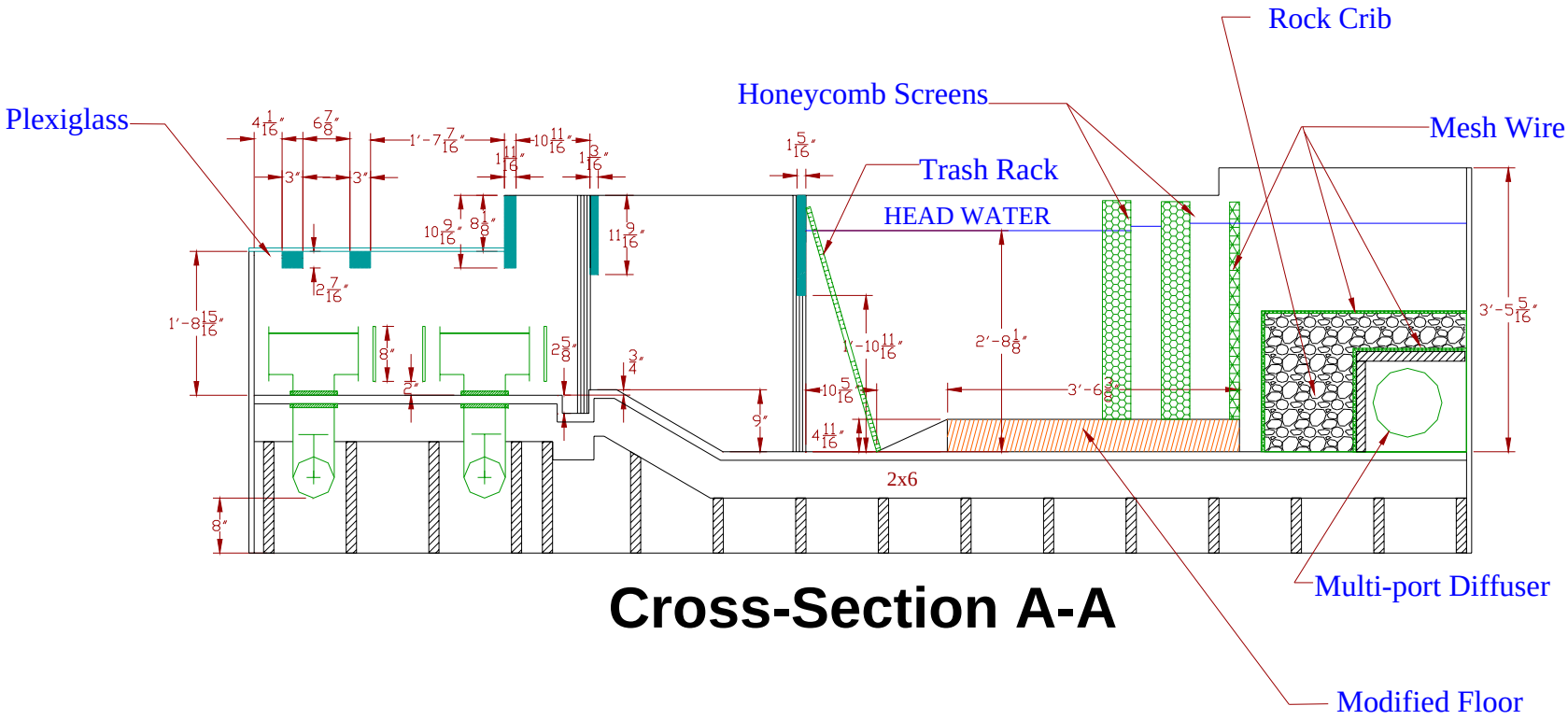

Revised with New Floor Added to the Approach Channel

Figure 10. A longitudinal cross-section of the model after modifying the head tank and raising the bed elevation by 4 11/16 inches (5.5 feet for the prototype).

Figure 11. View of the modified head box, looking downstream.

Figure 12. To dissipate the large eddies formed in the head box, wire mesh and two honeycomb screens were installed downstream of the rock crib.

Figure 13. The elbow meter consisting of a Meriam manometer and two pressure taps on the 12-inch water supply line was used to measure the total flow rate.

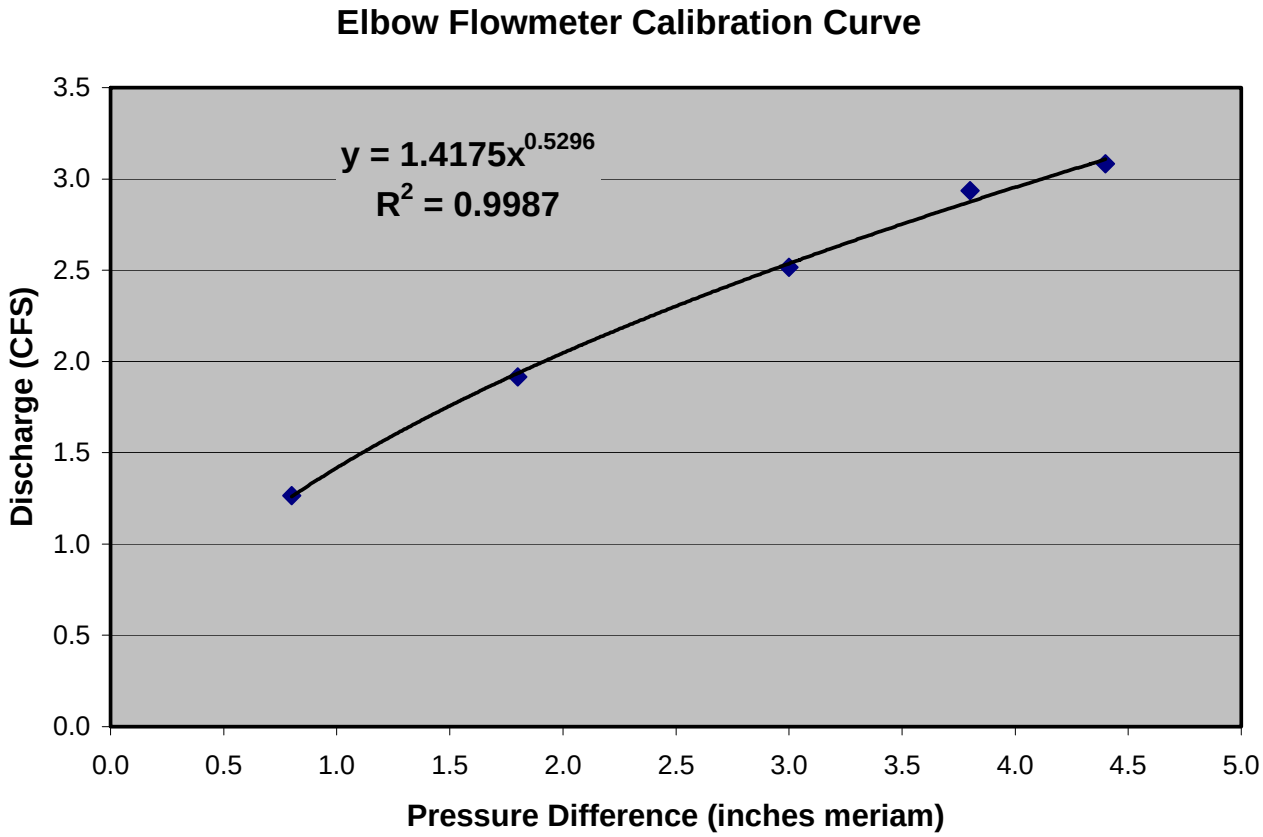

Figure 14. The elbow meter rating curve.

3. Model Runs and Results

After appropriate model adjustments were completed, two series of tests were conducted. The first test series was conducted using a trash rack with openings sized to represent 1.75-inch clear spacing in the prototype (full-scale), and the second series with openings of 1 inch clear spacing. Each series of tests consisted of velocity measurements at 40 locations taken at points corresponding to locations approximately one foot upstream of the trash rack in the full scale (prototype) intake. Three flow conditions were tested: 1300 cfs (representing typical flow through the project's 3 larger generating units) 1000 cfs (representing typical flow through the project's 5 smaller generating units), and 2170 cfs (representing maximum flow possible through the project's largest single generating unit).

The trash rack was installed at an inclined orientation of 3.2 (V) to 1(H). With this orientation, the toe of the trash rack was placed at the downstream end of the sloped section of the river bed, upstream of the intake structure (see Figure 10).

3.1. Modeling of Trash Rack

To size the trash rack in a physical model study, it is necessary to accurately simulate the head loss across the trash rack. The head loss is due to flow separation downstream of the vena contracta, which is the sudden contraction inside the opening of the trash rack. The depth of the trash rack has an insignificant contribution to the total head loss; however, it can cause an additional flow loss due to separation downstream of the trash rack. Head loss can be estimated using the following equation

$$h_l = K \frac{V^2}{2g} \tag{1}$$

where h_l is the head loss in ft, V is approach velocity in fps, g is the gravitational acceleration in ft/sec^2 and K is the dimensionless coefficient of head loss. The coefficient of head loss varies with Reynolds number ($\mathrm{Re} = \frac{VD}{\nu}$, where D is a length scale and ν is the kinematic viscosity of water). When the flow is turbulent, and the Reynolds number exceeds 5000, the head loss coefficient becomes more or less independent of the Reynolds number (Stefan and Fu, 1978). If

the flow regime through the trash rack opening in the model study is turbulent and the Reynolds number is about 5000 or more, then as the model K-value approaches the prototype K-value, the model trash rack hydraulically behaves similarly to the prototype trash rack.

Previous studies have been conducted to determine the head loss coefficient, *K*, of trash racks. Most studies have shown that at high Reynolds number, *K* is solely dependent upon the percentage opening of the trash rack and the coefficient of contraction.

Escande (1940) gave the following equation for the coefficient of head loss:

$$K = \left(\frac{1}{C_c - 1}\right)^2 \left(1 + \frac{s}{b}\right)^2 + \left(\frac{s}{b}\right)^2 \tag{2}$$

where C_c is the coefficient of contraction, *b* is the width of the opening and *s* is the distance from center-to-center of two adjacent bars. Coefficient of contraction, C_c, can be determined from equation 3 as follows

$$C_c = 0.54 + 0.1\sqrt{s/b} \tag{3}$$

Even though Escande's equation does not apply to trash racks with angles of attack different from 90 degrees, which is the case at the Prairie du Sac intake structure, it is evident that as long as the model trash rack has an *s/b* ratio similar to the prototype trash rack, and as long as the Reynolds number stays fairly high in the model, the trash rack will be modeled accurately.

3.2. Trash Rack with 1.75-inch Openings

A series of tests was performed on a trash rack model simulating prototype (full-scale) dimensions of a 1.75-inch opening, 3/8-inch bar thickness and 4-inch bar depth, which would result in a 68% open area excluding the structural components of the trash rack. The screen used for this test series had a 1 ¼ -inch opening, 1/4 -inch bar thickness and a 1-inch bar depth. Table 1 gives the prototype and model values of the parameters associated with the trash rack under 1300 cfs flow conditions. These values indicate that fully turbulent flow conditions and full similarity of head losses has been achieved in the model.

Table 1. Prototype and model parameter values of a trash rack with 1.75-inch openings, under 1300 cfs.

		Prototype	**Model**
Q	Flow (cfs)	1300	1.77
b	Opening (inch)	1.75	1.25
s	Bar thickness (inch)	0.38	0.25
C_c	Contraction coefficient	0.76	0.76
K	**Escande's equation**	0.20	0.18
H	Height (ft)	37.50	2.68
W	Width (ft)	40.50	2.89
N_1	Number of openings along the width	211	21
N_2	Number of openings along the height	228	23
q	Flow through each opening (cfs)	0.027	0.0037
Re		54115	32419

Velocities were measured at eight locations at each of five depths, which represented full-scale depths of 3.2, 10.5, 17.5, 28.8 and 31.7 feet above the river bed (total 40 points). Figures 15, 16, and 17 show the x-component (x being the main flow direction) of the velocity measurements for the 1300-cfs, 1000-cfs, and 2170-cfs flow conditions, respectively. The vertical lines in these figures represent the position of the piers.

For the 1300-cfs flow condition, velocities were relatively uniform across both the width and depth (Figure 15). Only velocities near the surface were reduced to the pressure of the ice wall behind the trash rack. Velocity measurements for the 1000-cfs flow condition were similar in distribution but low in magnitude as expected (Figure 16). The maximum measured velocity for these two flow conditions was 1.1 fps. Through-flow velocity associated with measured approach velocity was estimated for the 1300-cfs (typical) flow condition using the coefficient of contraction described in a previous section of this report. For the 1.75-inch opening trash rack, maximum through-flow velocity was estimated to be at 1.9 fps.

For the 2170-cfs flow condition (Figure 17), velocities were relatively uniform across the width, except at 31.7 feet (full-scale equivalent) from the riverbed, i.e. near the water surface. The largest standard of error (0.1 fps) was at a point located about 8 feet from the center of the left pier, looking upstream. The anomaly observed in the velocity measured at that location could be

due to an accumulation of debris in the honeycomb screens. The maximum measured approach velocity for the 2170-cfs flow condition was 1.9 fps.

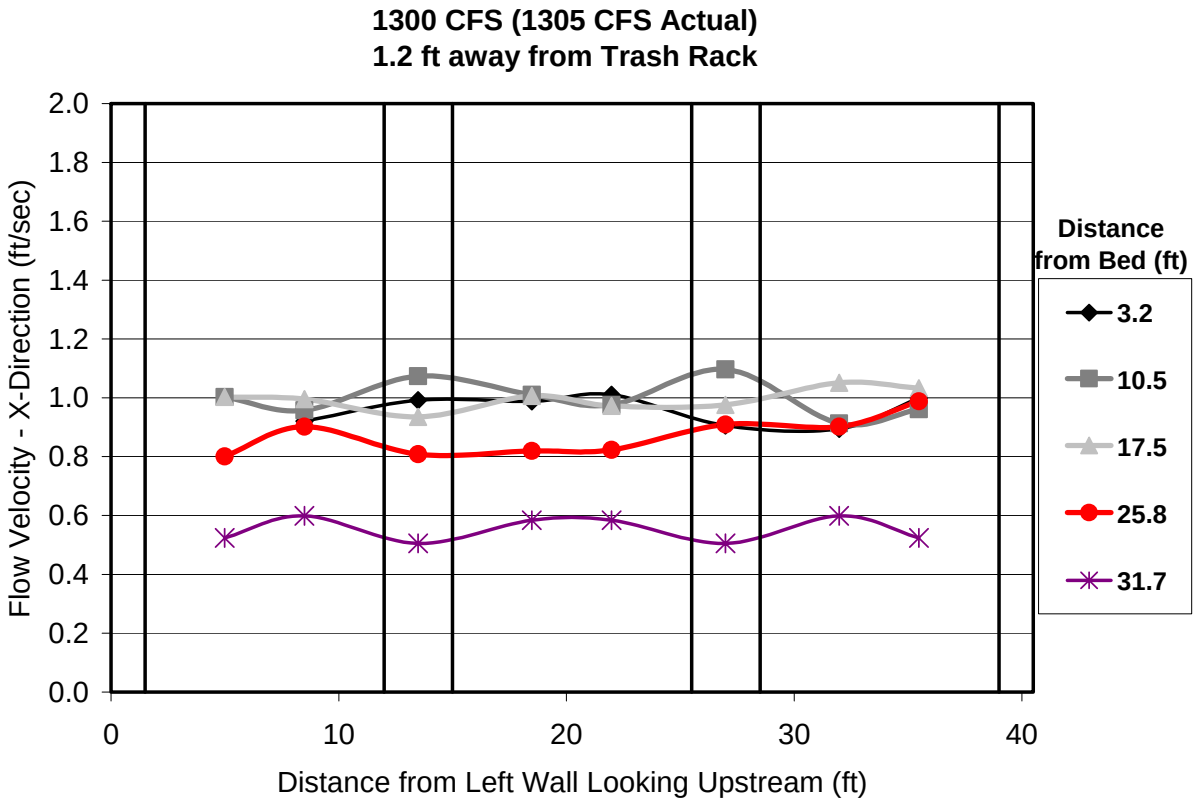

Figure 15. The x-component of the velocity measured at 40 locations, 1.2 ft away from a trash rack with 1.75-inch openings, under the 1300 cfs flow condition. The actual measured flow was 1305 cfs. Vertical lines show the position of the piers.

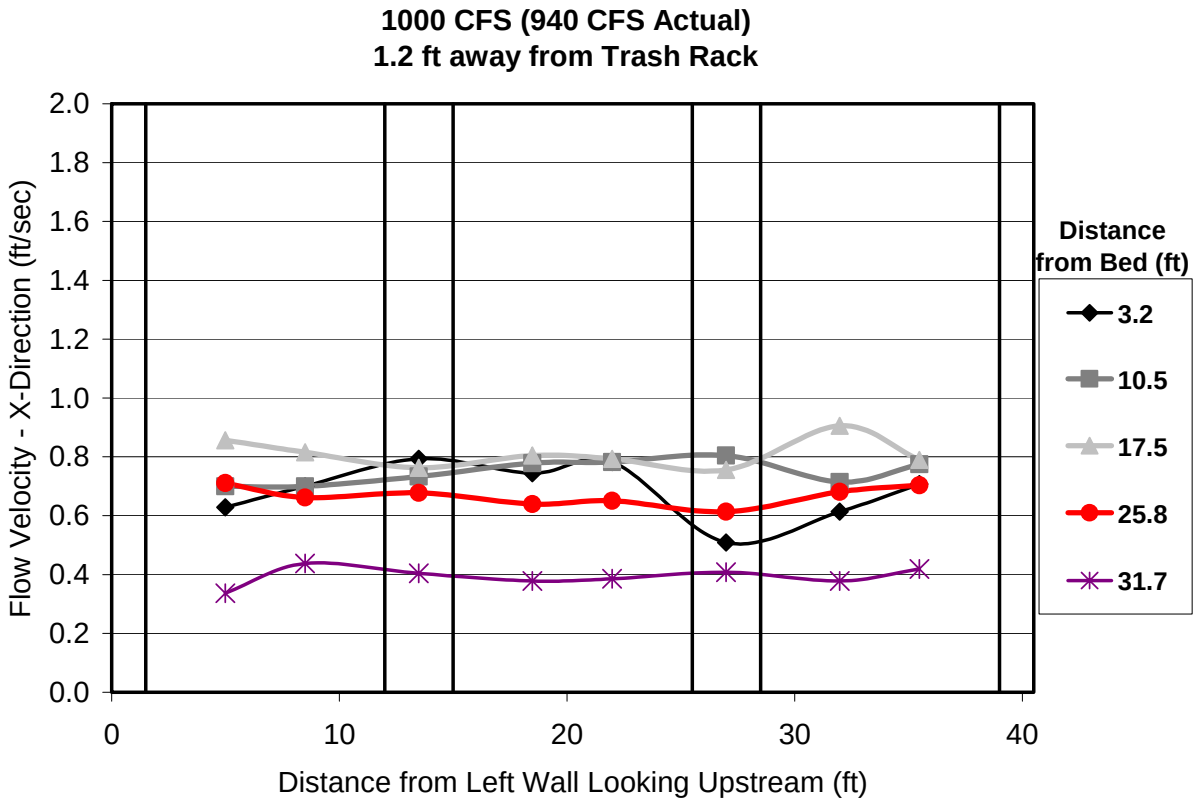

Figure 16. The x-component of the velocity measured at 40 locations, 1.2 ft away from a trash rack with 1.75 inch openings, under the 1000 cfs flow condition. The actual measured flow was 940 cfs. Vertical lines show the position of the piers.

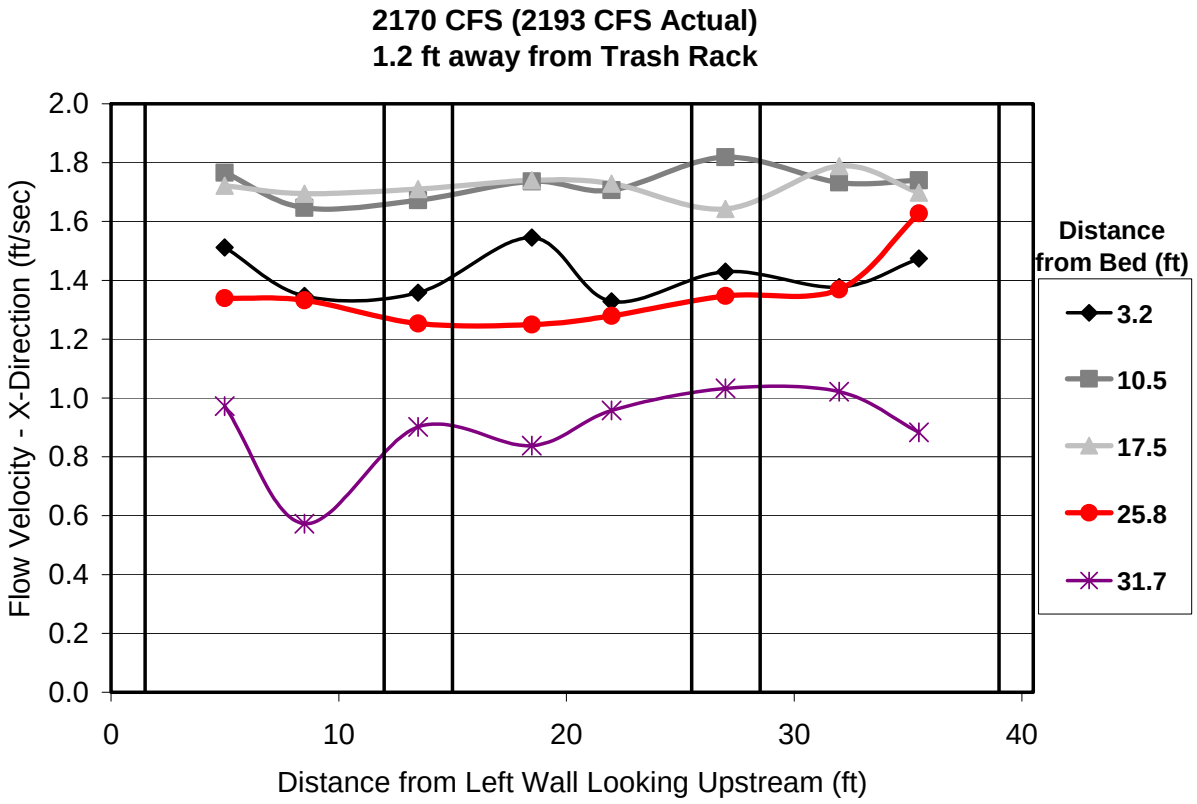

Figure 17. The x-component of the velocity measured at 40 locations, 1.2 ft away from a trash rack with 1.75-inch openings under the 2170 cfs flow condition. The actual measured flow was 2193 cfs. Vertical lines show the position of the piers.

3.3. Trash Rack with 1.0-inch Openings

The second test series was performed with a trash rack model simulating prototype (full-scale) dimensions of 1.0-inch openings, 3/8-inch bar thickness and 4-inch bar depth, which would result in a 53% open area excluding the structural components of the trash rack. The screen used for this series of tests had a 0.5-inch opening, 3/16-inch bar thickness and a 0.32-inch bar depth. Table 2 gives the prototype and model values of the parameters associated with this trash rack.

Table 2. Prototype and model parameter values of a trash rack with 1.0-inch openings, under 1300 cfs.

		Prototype	**Model**
Q	Flow (cfs)	1300	1.77
b	Opening (inch)	1.00	0.50
s	Bar thickness (inch)	0.38	0.19
C_c	Contraction coefficient	0.70	0.70
K	**Escande's equation**	0.48	0.48
h	Height (ft)	37.50	2.68
w	Width (ft)	40.50	2.89
N1	Number of openings along the width	327	46
N2	Number of openings along the height	353	50
q	Flow through each opening (cfs)	0.011	0.0008
Re		45608	27323

Velocities were measured at the same eight locations as for the 1.75-inch-opening trash racks. Figures 18, 19, and 20 show the x-component of velocity measurements for the 1300-cfs, 1000-cfs, and 2170-cfs flow conditions. For the 1300-cfs flow condition, the maximum velocity measured was 1.2 fps. Some irregularity was observed in velocity distributions for this test, which may have resulted from debris accumulation. As previously noted, the model utilized Mississippi River water, which carries debris that can accumulate in model areas such as the honeycomb screens upstream of the model intake. Through-flow velocity associated with measured approach velocity was estimated for the 1300-cfs (typical) flow condition using the coefficient of contraction described in a previous section of this report. For the 1.0-inch opening trash rack, maximum through-flow velocity was estimated to be at 2.4 fps.

Test results were more uniform for the 1000-cfs flow condition. As shown in Figure 19, the maximum measured velocity was 0.8 fps.

Figure 20 shows test results for the 2170-cfs flow condition. For this round of tests, a repeatability test was performed to verify the model and measurement procedure (see Figure B.1). The velocities show little variation from Test 1 to Test 2, indicating the tests were repeatable. The maximum velocity did not exceed 1.7 fps under the 2170 cfs flow condition.

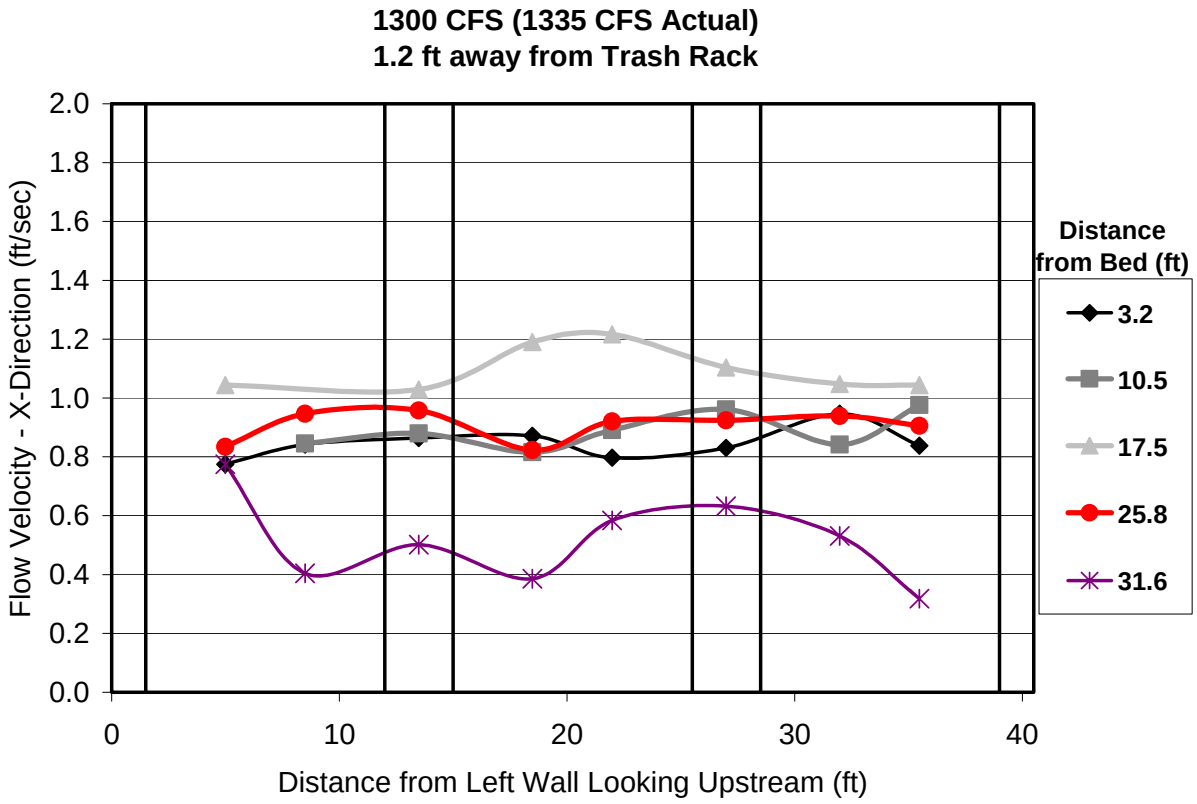

Figure 18. The x-component of the velocity measured at 40 locations, 1.2 ft away from a trash rack with 1.0-inch openings, under the 1300 cfs flow condition. The actual measured flow was 1335 cfs. Vertical lines show the position of the piers.

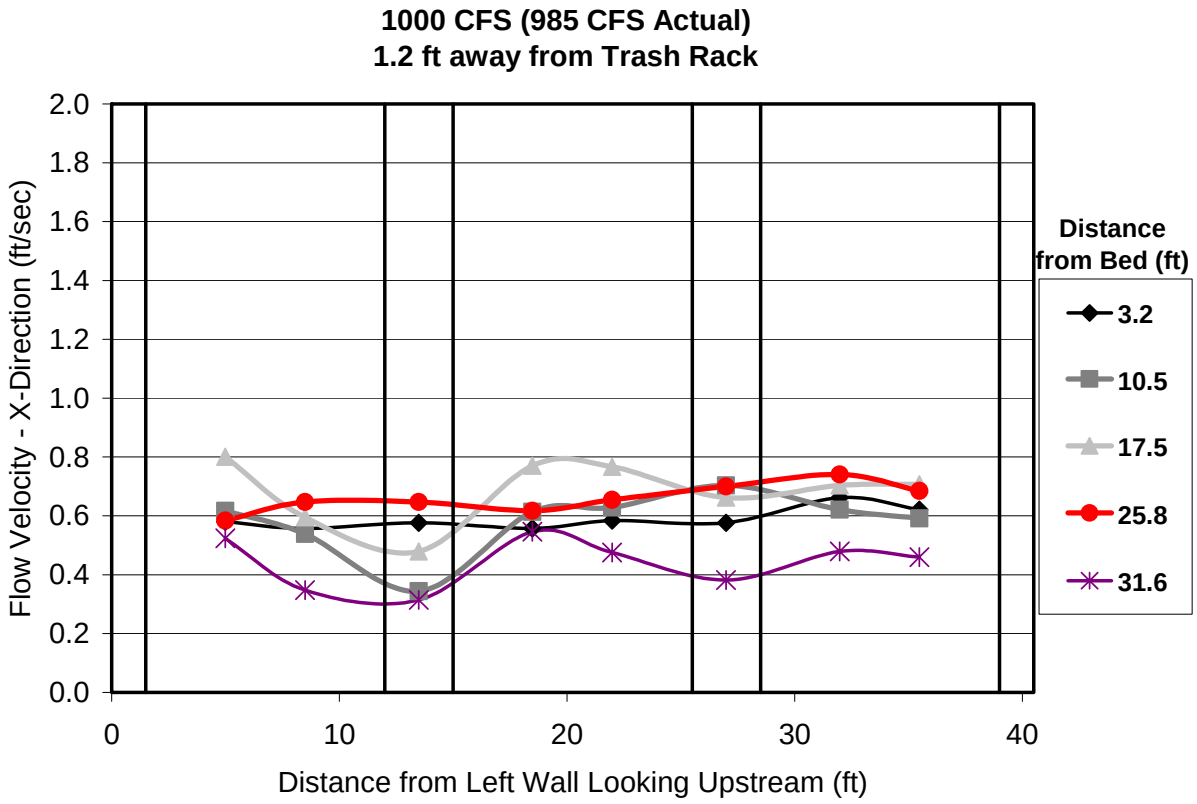

Figure 19. The x-component of the velocity measured at 40 locations, 1.2 ft away from a trash rack with 1.0-inch openings, under the 1000 cfs flow condition. The actual measured flow was 985 cfs. Vertical lines show the position of the piers.

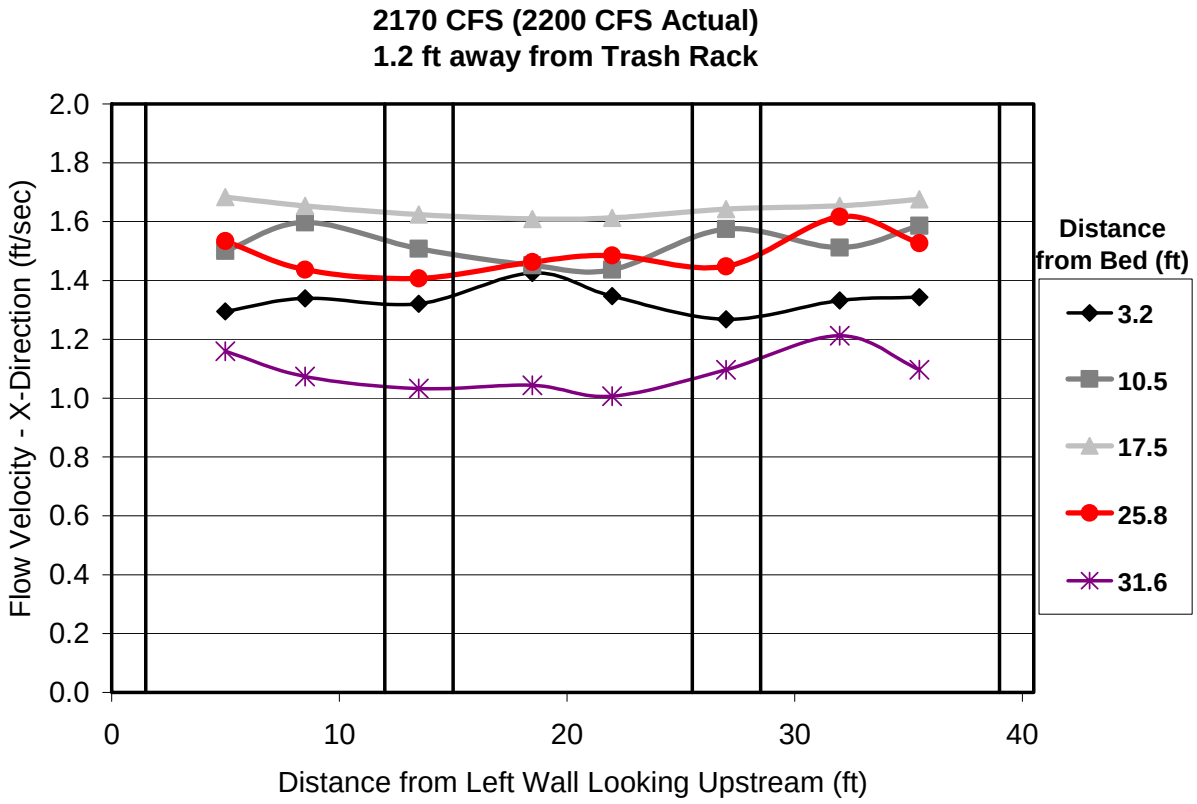

Figure 20. The x-component of the velocity measured at 40 locations, 1.2 ft away from a trash rack with 1.0-inch openings, under the 2170 cfs flow condition. The actual measured flow was 2200 cfs. Vertical lines show the position of the piers.

4. Summary

The physical model of a single unit of the intake structure of the Prairie du Sac Hydroelectric Project was built and tested at the St. Anthony Falls Laboratory. The model was built at a scale of 1 to 14.

In the model study the existing trash rack inside the intake structure was replaced with a trash rack upstream of the structure and approach velocity characteristics were evaluated for new conditions. Two trash rack configurations were studied: a trash rack with 1.75-inch openings (68% opening), and a trash rack with 1.0-inch openings (53% opening)

Flow velocities were measured at 40 locations in the model, selected to correspond to points located approximately one foot upstream from the trash rack in the full-scale (prototype) structure, using a 3-dimentional ADV.

Tests were conducted under three flow conditions: 1300 cfs (representing typical flow through the project's 3 larger generating units); 1000 cfs (representing typical flow through the project's 5 smaller generating units); and 2170 cfs (representing maximum flow through the project's largest single generating unit). Under the 1300 cfs flow condition, the approach flow velocities did not exceed 1.1 and 1.2 fps with the 1.75- and 1.0-inch opening trash racks, respectively. The maximum through flow velocities for the 1300 cfs flow condition were estimated to be 1.9 and 2.4 fps, respectively. Under the 1000 cfs flow condition, maximum approach velocities did not exceed 1 and 0.8 fps with 1.75- and 1.0-inch opening trash racks, respectively. Under the 2170 cfs flow condition, the approach flow velocities did not exceed 1.7 fps and 1.9 fps with the 1.75- and 1.0-inch opening trash racks, respectively.

References

Escande, L., 1944. Expressiom de la perte de charge a la traversee d’un grille, in Montes, S., 1998. *Hydraulics of Open Channel Flow*. ASCE Press, PP 399-340.

Stefan, H. G., and Fu, A., 1978. Headloss Characteristics of Six Profile-Wire Screen Panels. *St. Anthony Falls Laboratory, Project Report No. 175*, pp 70.

Appendix A: Longitudinal Profiles of the River Bed Upstream of the Intake

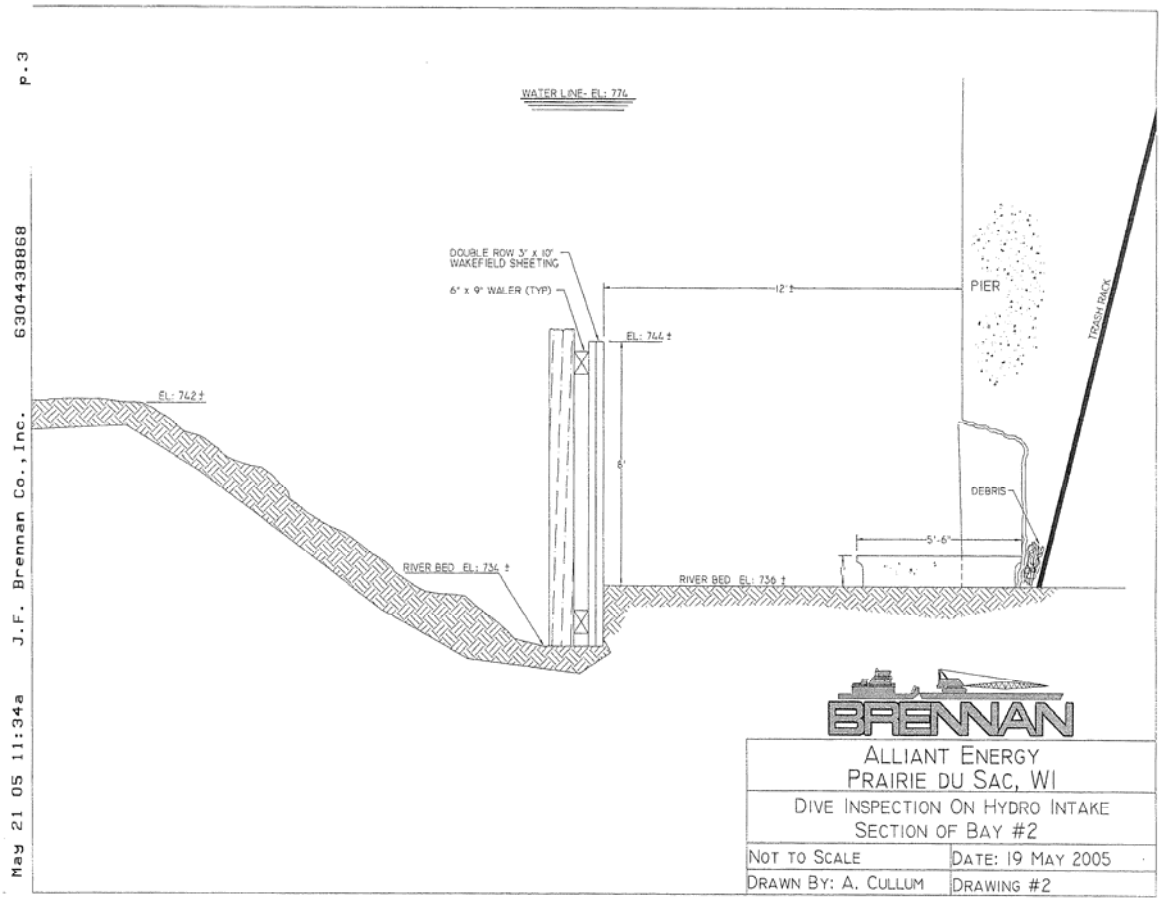

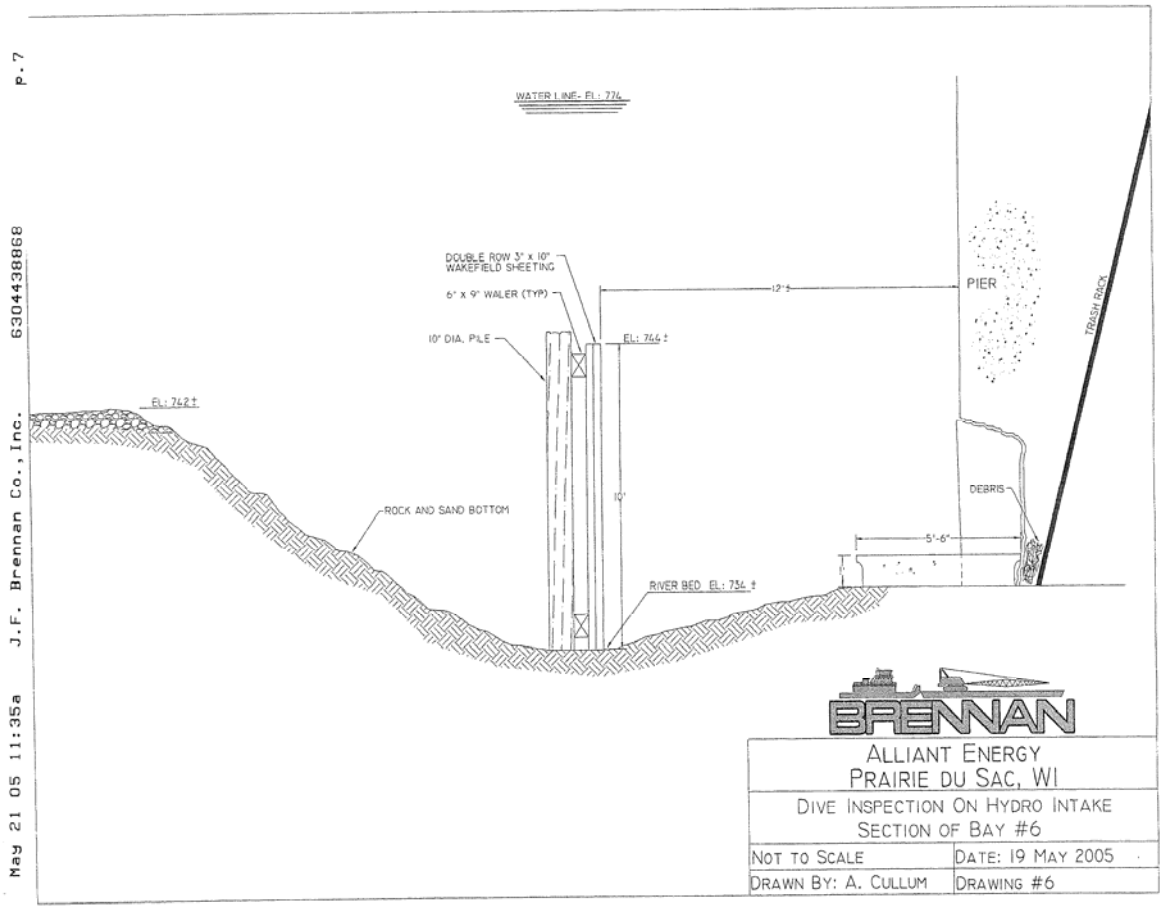
WATER LINE- EL: 774
DOUBLE ROW 3" x 10" WAKEFIELD SHEETING
6" x 9" WALER (TYP)
10" DIA. PILE
12'±
EL: 744±
PIER
TRASH RACK
EL: 742±
ROCK AND SAND BOTTOM
10'
DEBRIS
5'-6"
RIVER BED EL: 734 ±
BRENNAN
ALLIANT ENERGY
PRAIRIE DU SAC, WI
DIVE INSPECTION ON HYDRO INTAKE
SECTION OF BAY #6
NOT TO SCALE
DATE: 19 MAY 2005
DRAWN BY: A. CULLUM
DRAWING #6

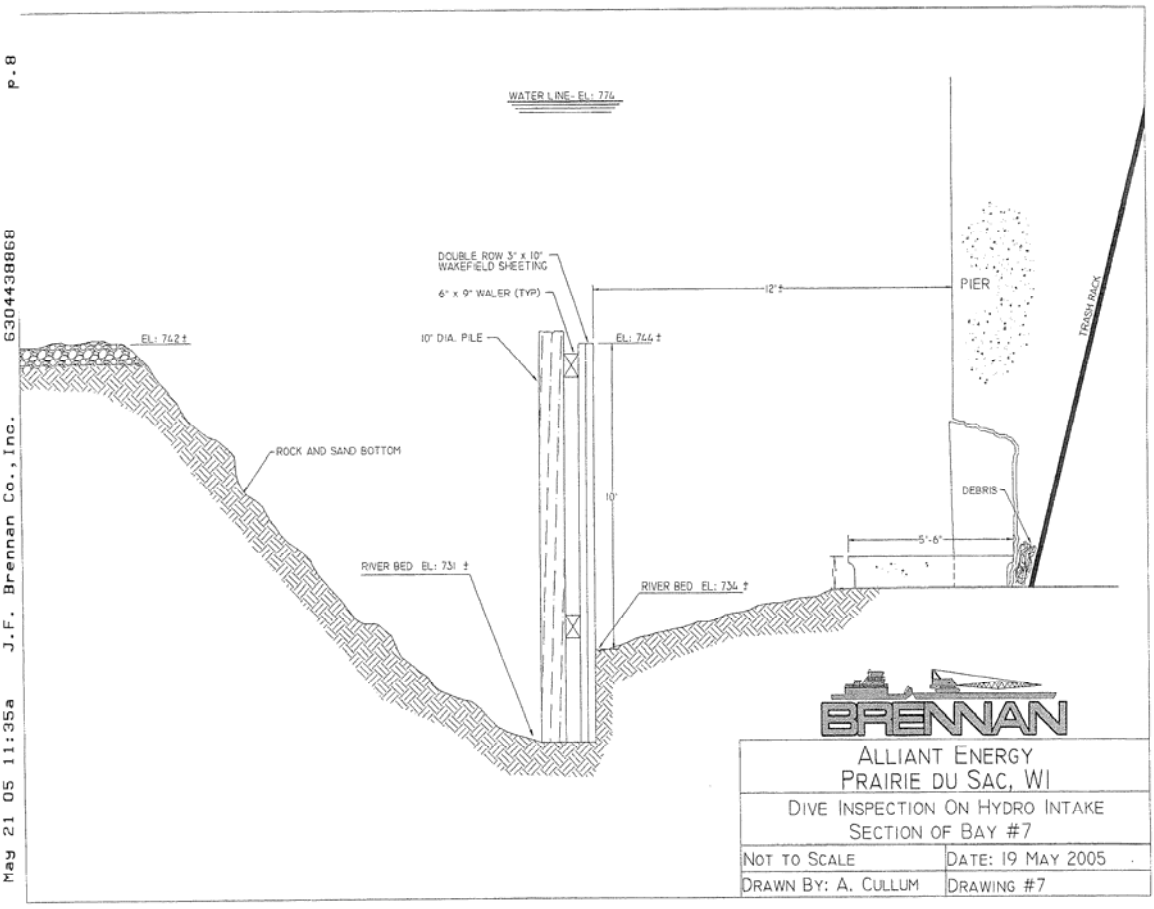
WATER LINE- EL.: 776
DOUBLE ROW 3" x 10" WAKEFIELD SHEETING
6" x 9" WALER (TYP)
10" DIA. PILE
12"±
PIER
TRASH RACK
EL.: 742±
EL.: 744±
ROCK AND SAND BOTTOM
10'
DEBRIS
5'-6"
RIVER BED EL.: 731 ±
RIVER BED EL.: 734 ±
BRENNAN
ALLIANT ENERGY
PRAIRIE DU SAC, WI
DIVE INSPECTION ON HYDRO INTAKE
SECTION OF BAY #7
NOT TO SCALE
DATE: 19 MAY 2005
DRAWN BY: A. CULLUM
DRAWING #7

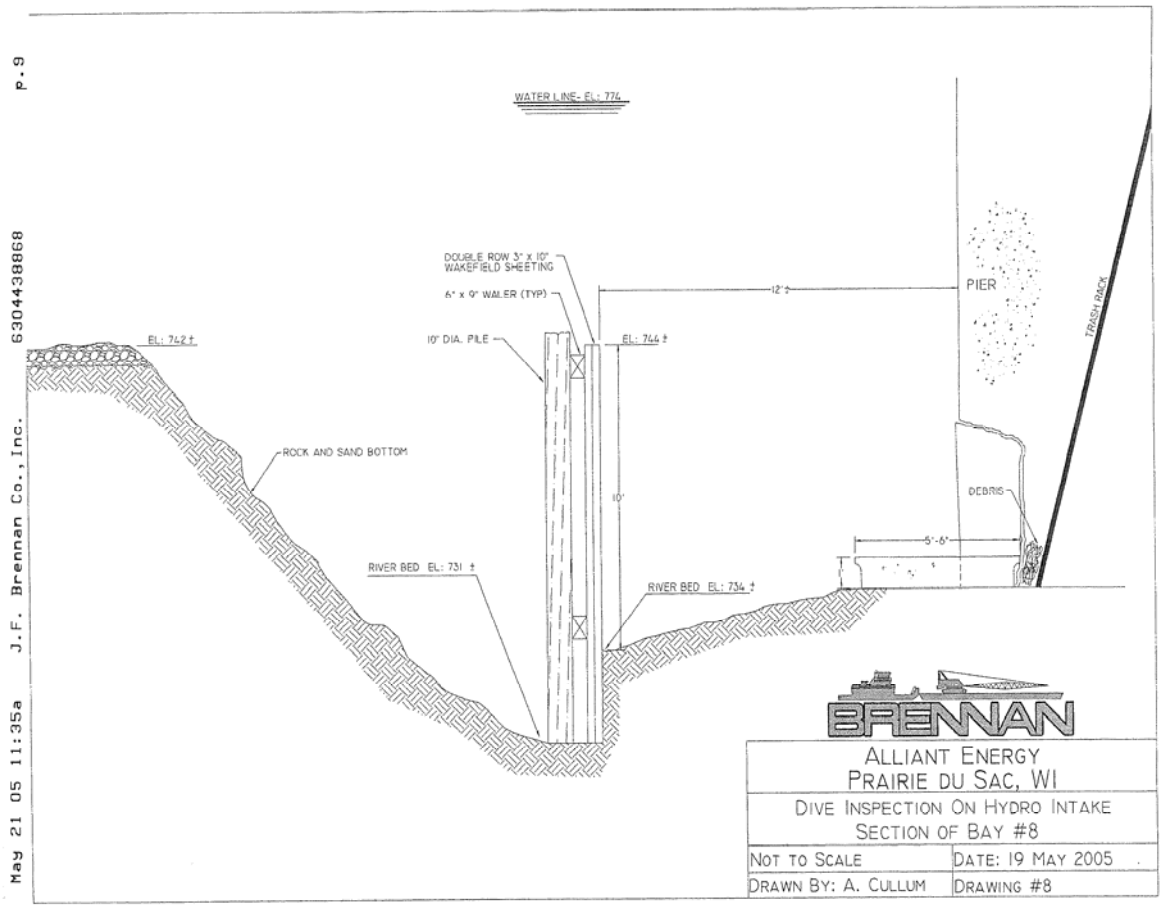
WATER LINE- EL.: 774
DOUBLE ROW 3" x 10" WAKEFIELD SHEETING
6" x 9" WALER (TYP)
10" DIA. PILE
12'±
PIER
TRASH RACK
EL: 742±
EL: 744±
ROCK AND SAND BOTTOM
10'
DEBRIS
5'-6"
RIVER BED EL: 731 ±
RIVER BED EL: 734 ±
BRENNAN
ALLIANT ENERGY
PRAIRIE DU SAC, WI
DIVE INSPECTION ON HYDRO INTAKE
SECTION OF BAY #8
NOT TO SCALE
DATE: 19 MAY 2005
DRAWN BY: A. CULLUM
DRAWING #8

Appendix B: Repeatability Test

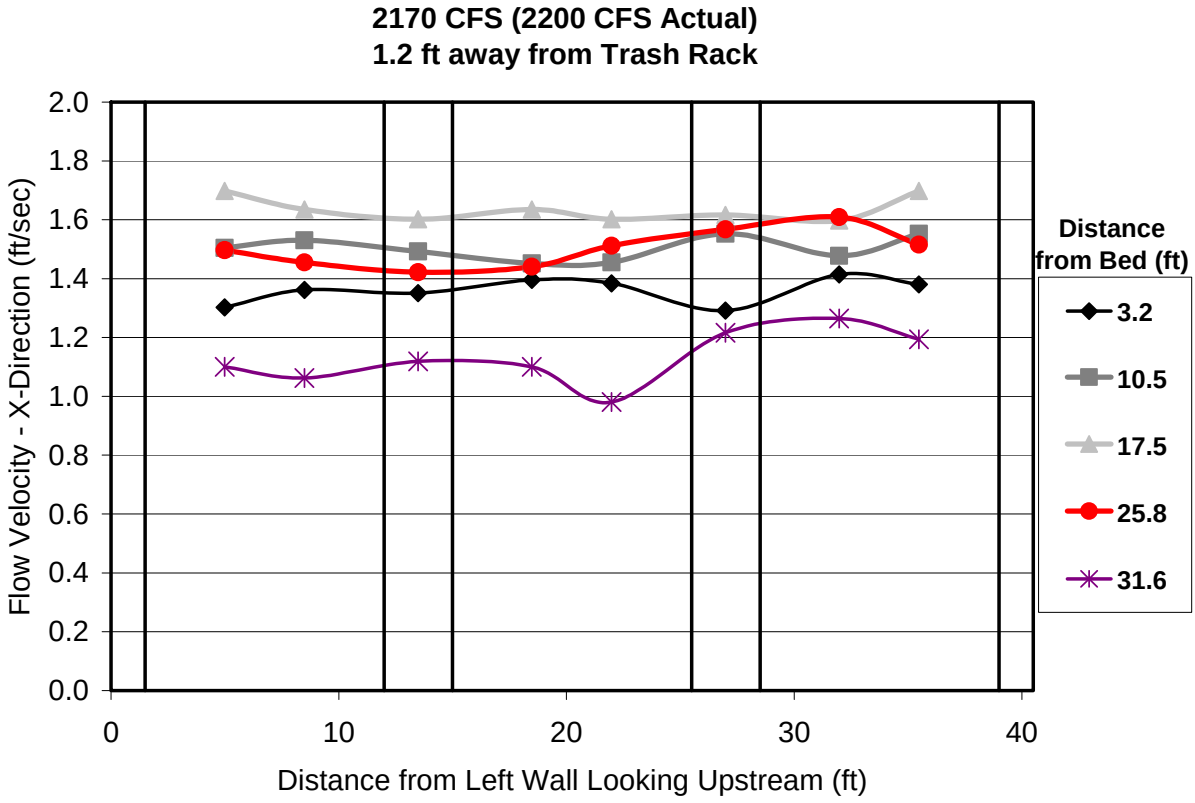

Figure B.1. The x-component of the velocity measured at 40 locations, 1.2 ft away from a trash rack with 1.0-inch openings, under the 2170 cfs flow condition. The actual measured flow was 2200 cfs. This was a repeatability test for the test shown in Figure 20.

Appendix C: New Test Series with Trash Racks at the Existing Location

After the test series were conducted for two different trash rack openings upstream of the intake structure, Mead & Hunt decided to explore the flow conditions between the ice-wall and the trash rack with various trash racks at the existing location. The new test series were similarly conducted under three flow conditions and two trash rack openings. These test series included velocity measurements and flow visualization. The flow visualization would show whether whirlpool or eddy effects occur between the trash rack and the ice-wall that could affect fish movement.

In order to visualize flow, one of the outside walls of the bay area was replaced by a Plexiglas wall (Figure C.1). The flow patterns were observed by injecting red dye and confetti upstream of the ice-wall and were documented using a digital video camera.

Initially two test series were conducted: (1) with an ice-wall with 11 feet of submergence (existing condition) and a prototype trash rack with 1.75-inch clear openings, and (2) with an ice-wall with 11 feet of submergence and a prototype trash rack with 1.0-inch clear openings. Subsequently, 12 intermediate tests were conducted to decide upon the ideal submergence depth of a modified ice-wall. After these intermediate tests, two new test series were conducted: (1) with an ice-wall with three feet submergence and a prototype trash rack with 1.75-inch clear openings, and (2) with an ice-wall with three feet submergence and a prototype trash rack with 1.0-inch clear openings. The results of the tests are presented in the following sections.

In order to measure the velocity components in the bay area, especially between the ice-wall and the trash rack, the 3-D ADV was situated very close to the boundaries, i.e. the ice-wall and the bay walls. Therefore, the reflection of the sound waves emitted by the device resulted in recording very sporadic velocity values. To partially remedy the situation, the ADV was held 2.9 feet away from the trash rack unlike the previous test, where the ADV was held approximately one foot away from the trash rack. The quality of velocity measurements was improved but some variability in flow velocities was still evident.

All video clips documenting the flow patterns are stored in the CD enclosed in this report.

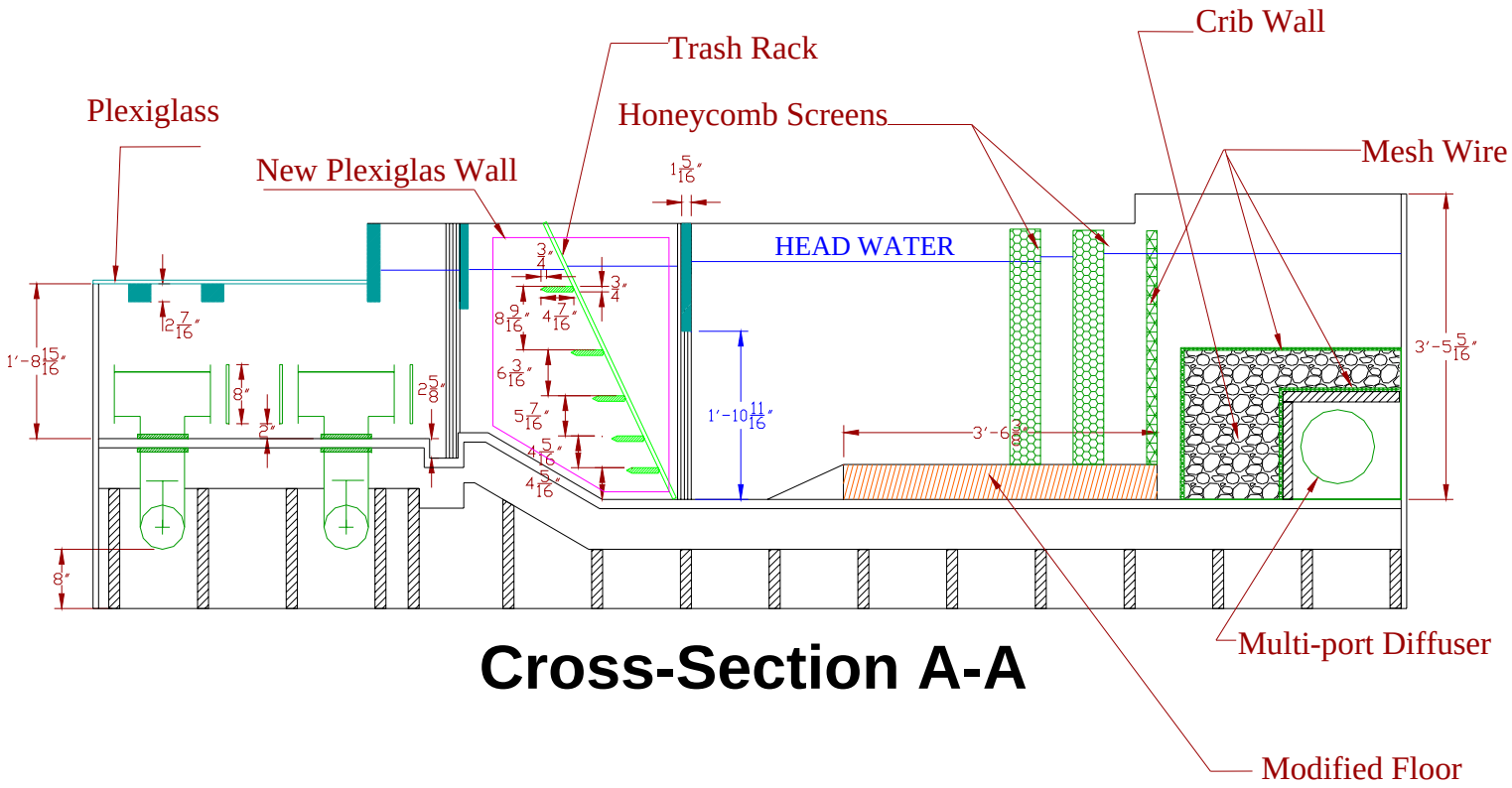

Revised with Existing Trash Rack

Figure C.1. A longitudinal cross-section of the model after replacing one of the outside walls with Plexiglas and placing the trash rack in its exiting location.

C.1. Test Series # 1: Existing Ice-Wall and Trash Rack with 1.75-inch Openings

In the first test series, the trash rack clear opening was 1.75 inches. Three tests were conducted under the following flow conditions: (1) 1000 cfs, (2) 1300 cfs, and (3) 2200 cfs. All three components of velocity were measured at 5 depths, and six locations at each depth, i.e. a total of 30 points. The y-component of velocity, which was perpendicular to the bay walls, was negligible, therefore, only the x- and z-components of flow velocity were plotted. In addition, the flow velocities were measured upstream of the intake structure, denoted as inlet flow in the figures, to check the uniformity of the approach flow towards the intake bay area.

The results of velocity measurements show that x-components of velocities were less than 2 fps under 1000 cfs flow condition (Figure C.2). The z-components of velocities were near zero everywhere except from the area near the ice-wall to the surface, indicating the presence of a strong eddy between the ice-wall and the trash rack (Figure C.3). The z-components of velocities in that region varied from 0.5 to 1.1 fps.

Under the 1300 cfs flow condition, the x-components of velocities exceeded 2 fps at about 26 ft from the bed, i.e. near the lower end of the ice-wall (Figure C.4). The maximum flow velocity occurs at the lower end of the ice-wall due to the contraction of the upper 10 feet of the approach flow. The variability observed in velocities measurements is mainly due to the reflection of the ADV sound waves in a confined space. The z-components of velocities from 26 ft from the bed did not exceed 1.5 fps (Figure C.5).

Under the 2200 cfs flow condition, at about 26 ft from the bed, the x-components of velocities exceeded 4 fps (Figure C.6), while the z-components exceeded 2 fps (Figure 7). More variability was evident in measured velocities due to highly turbulent flow conditions and measurements in a confined space.

The qualitative analysis of the dye study indicated the presence of persistent large eddies between the ice-wall and the trash rack due to flow separation. Under all three flow conditions, the dye would stay between the ice-wall and the trash rack long after the injection of the dye was stopped.

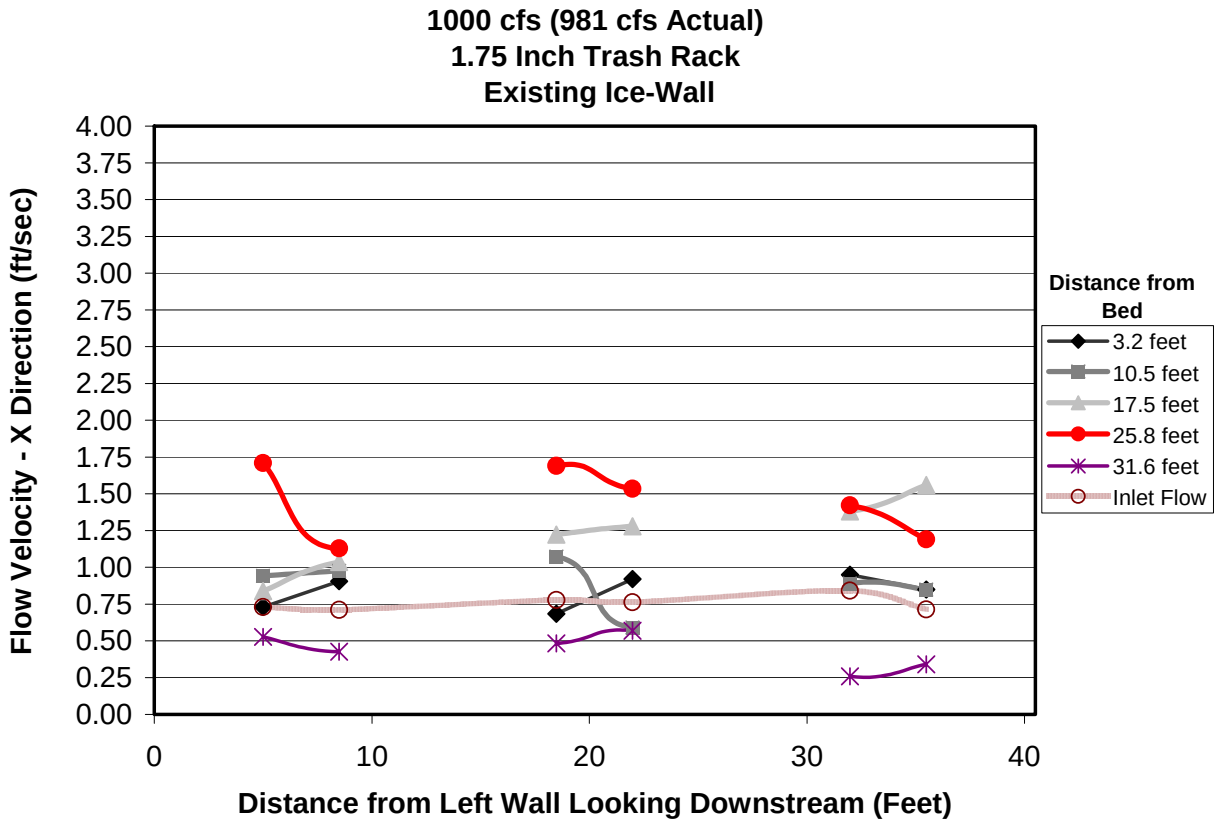

Figure C.2. The x-component of the velocity measured at 30 locations inside the bay areas, 2.9 ft away from a trash rack with 1.75-inch openings at its current location, under the 1000 cfs flow condition. The actual measured flow was 981 cfs.

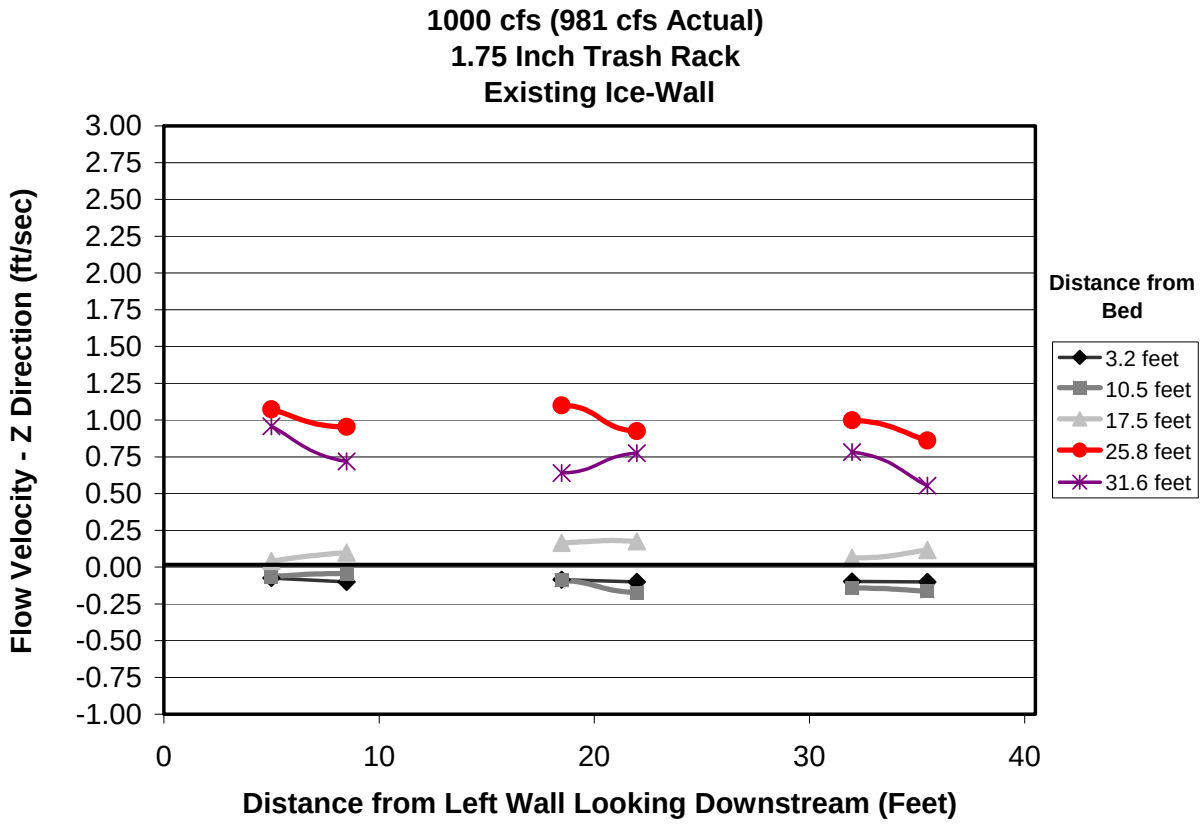

Figure C.3. The z-component of the velocity measured at 30 locations inside the bay areas, 2.9 ft away from a trash rack with 1.75-inch openings at its current location, under the 1000 cfs flow condition. The actual measured flow was 981 cfs.

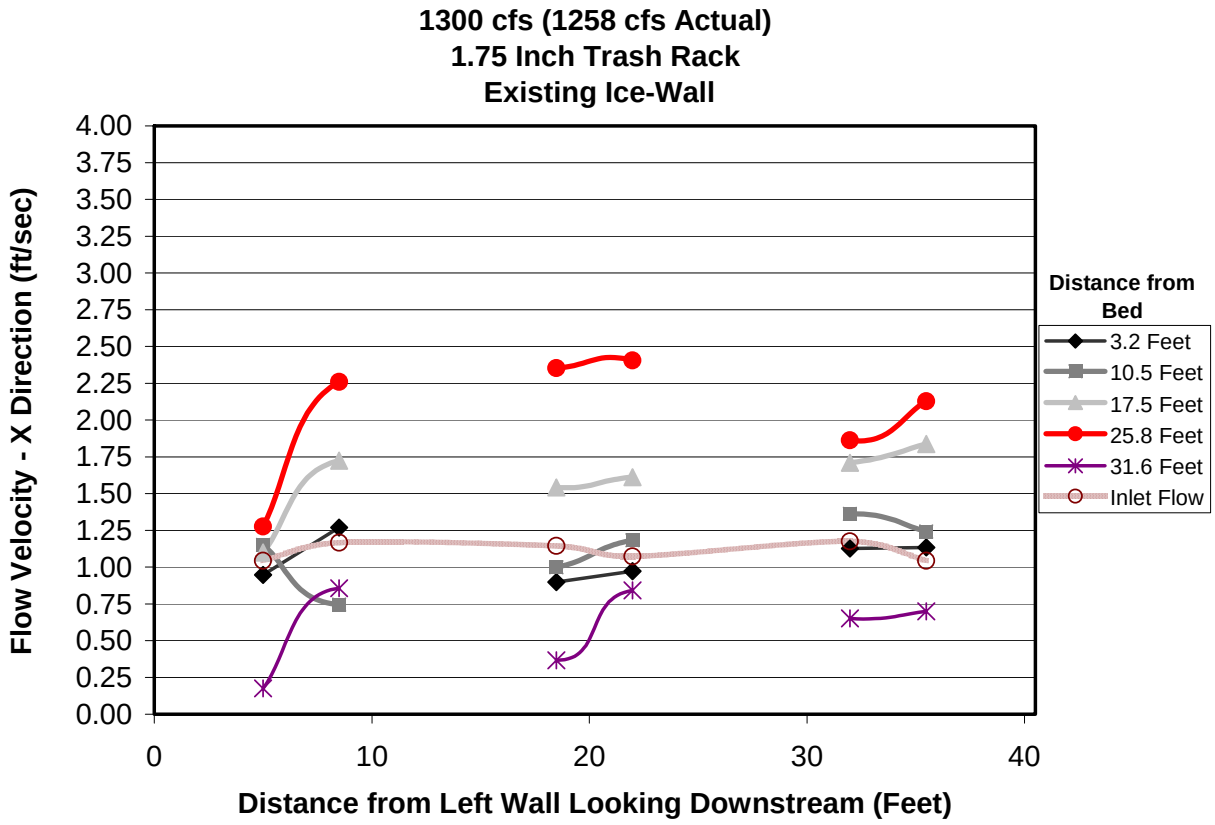

Figure C.4. The x-component of the velocity measured at 30 locations inside the bay areas, 2.9 ft away from a trash rack with 1.75-inch openings at its current location, under the 1300 cfs flow condition. The actual measured flow was 1258 cfs.

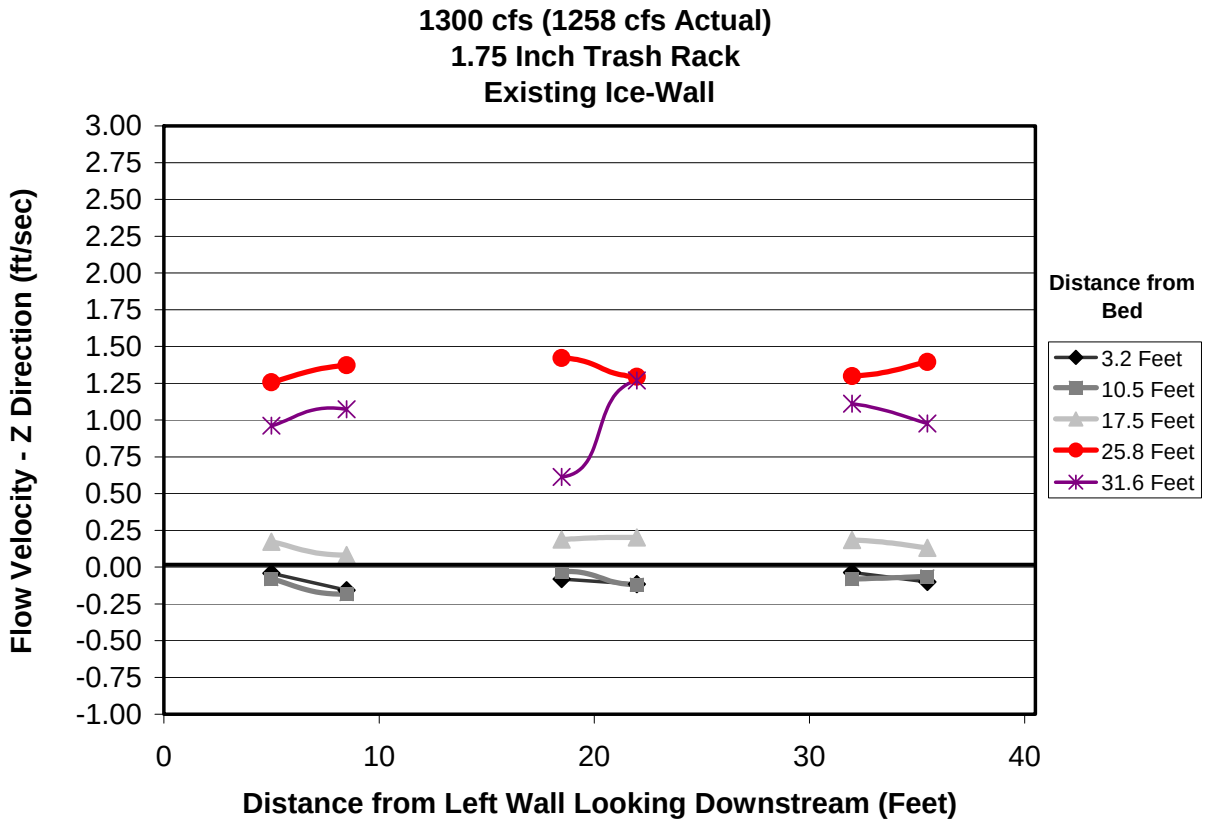

Figure C.5. The z-component of the velocity measured at 30 locations inside the bay areas, 2.9 ft away from a trash rack with 1.75-inch openings at its current location, under the 1300 cfs flow condition. The actual measured flow was 1258 cfs.

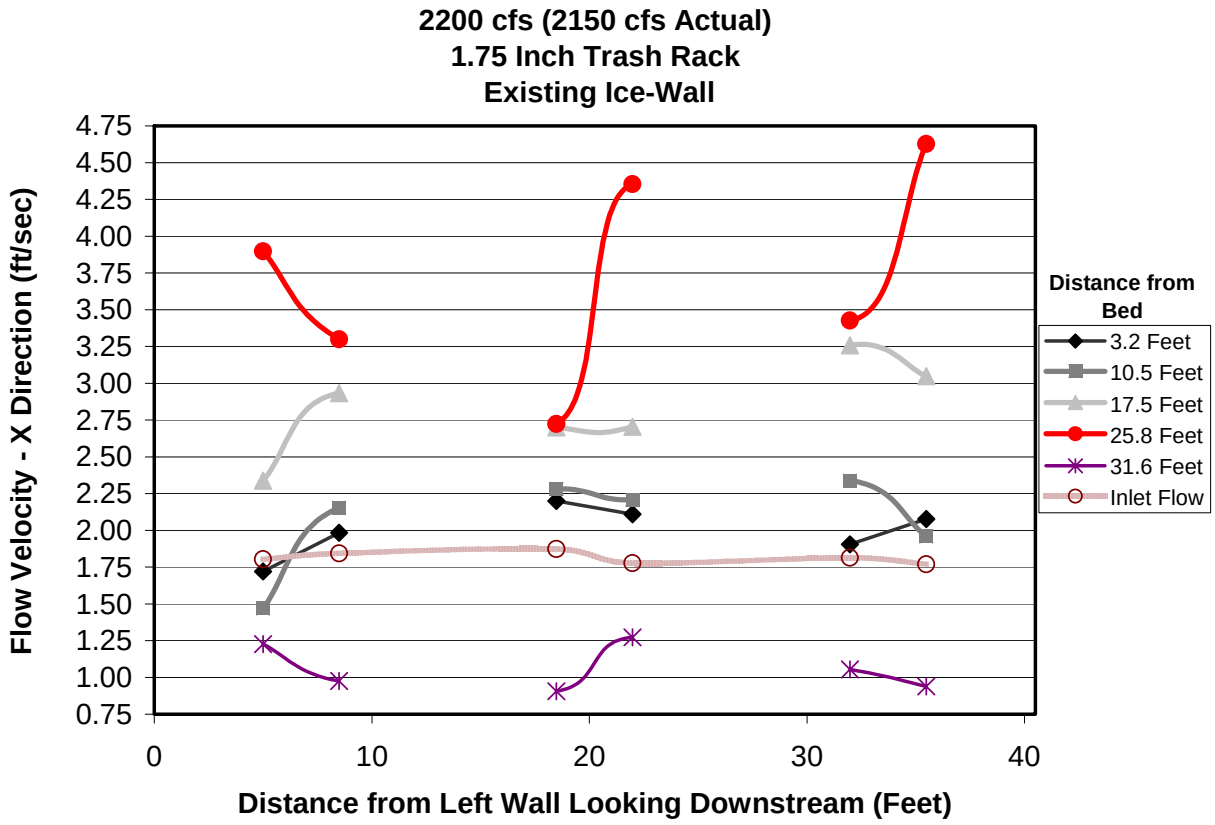

Figure C.6. The x-component of the velocity measured at 30 locations inside the bay areas, 2.9 ft away from a trash rack with 1.75-inch openings at its current location, under the 2200 cfs flow condition. The actual measured flow was 2150 cfs.

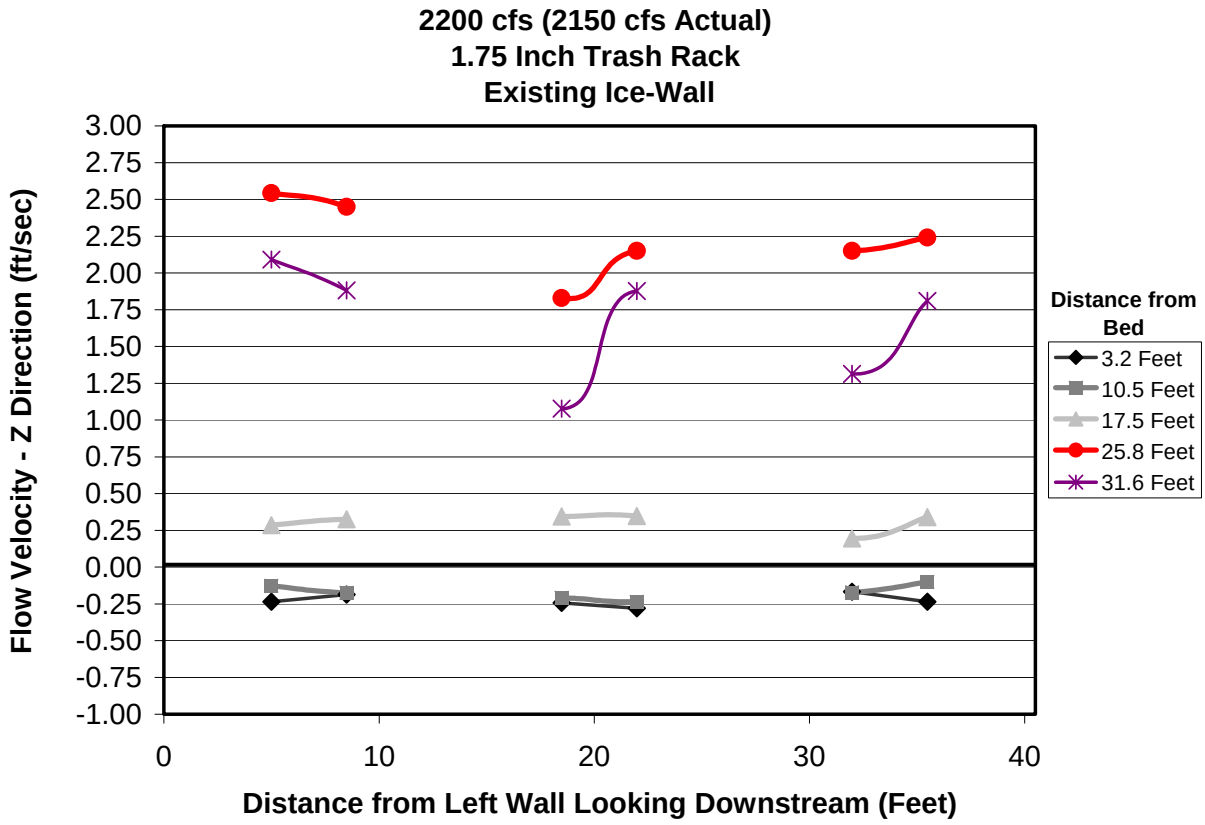

Figure C.7. The z-component of the velocity measured at 30 locations inside the bay areas, 2.9 ft away from a trash rack with 1.75-inch openings at its current location, under the 2200 cfs flow condition. The actual measured flow was 2150 cfs.

C.2. Test Series # 2: Existing Ice-Wall and Trash Rack with 1.0-inch Openings

In the second test series, the trash rack clear opening was 1.0 inch. The tests were conducted under the same flow conditions and velocity components were measured at the same locations.

Under the 1000 cfs flow condition, the x-components of velocities were less than 2 fps (Figure C.8) and the z-components did not exceed 1.25 fps (Figure C.9).

Under the 1300 cfs flow condition, at about 26 ft from the bed, near the lower end of the ice-wall, the x-components of velocities did not exceed 2.3 fps (Figure C.10) and the z-components did not exceed 1.5 fps (Figure C.11).

Under the 2200 cfs flow condition, at about 26 ft from the bed, the x-components of velocities did not exceed 3.6 fps (Figure C.12), and the z-components did not exceed 2.6 fps (Figure 13).

In comparison to the first test series, overall the velocities were more uniformly distributed across each depth, which was due to the smaller opening of the trash rack. Nevertheless, some variability was evident in measured velocities, which was due to the use of the ADV in a confined space.

The qualitative analysis of the dye study still indicated the presence of persistent large eddies between the ice-wall and the trash rack due to flow separation. Under all three flow conditions, the dye would stay between the ice-wall and the trash rack long after the injection of the dye was stopped.

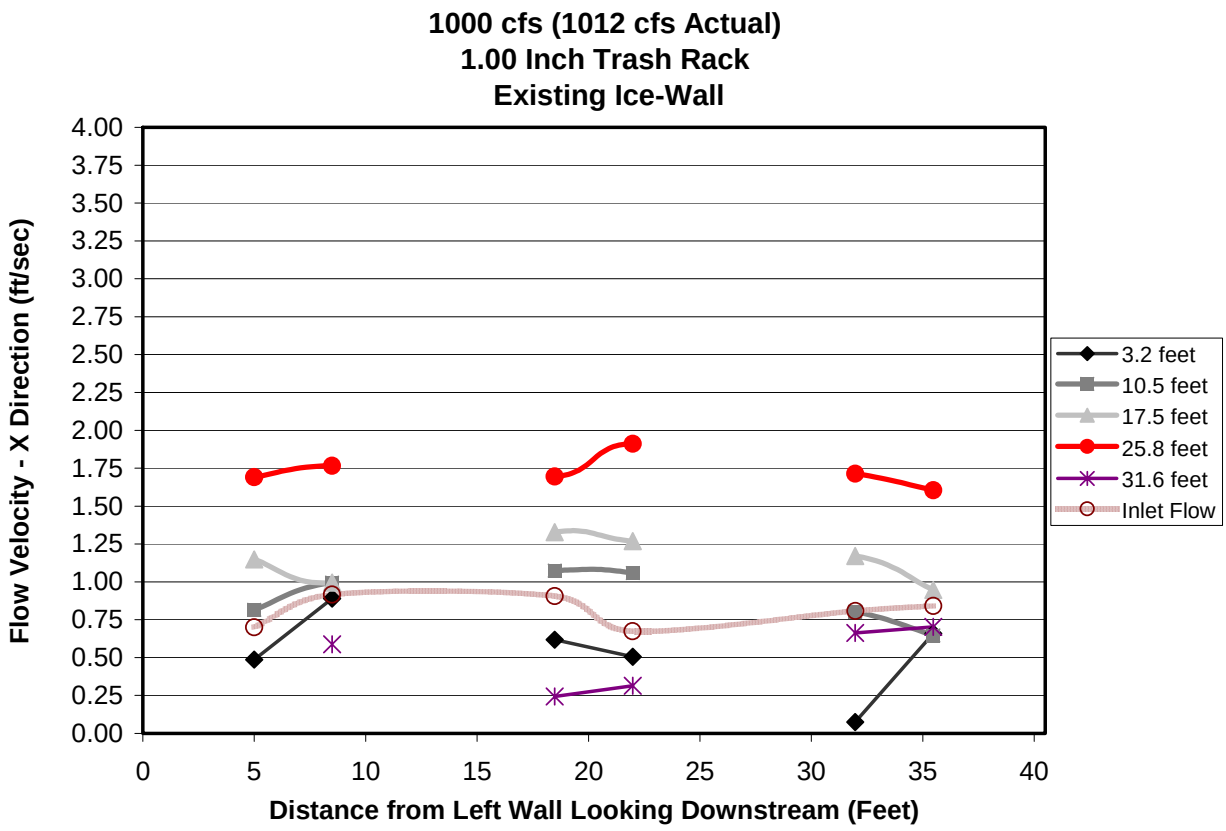

Figure C.8. The x-component of the velocity measured at 30 locations inside the bay areas, 2.9 ft away from a trash rack with 1.0-inch openings at its current location, under the 1000 cfs flow condition. The actual measured flow was 1012 cfs.

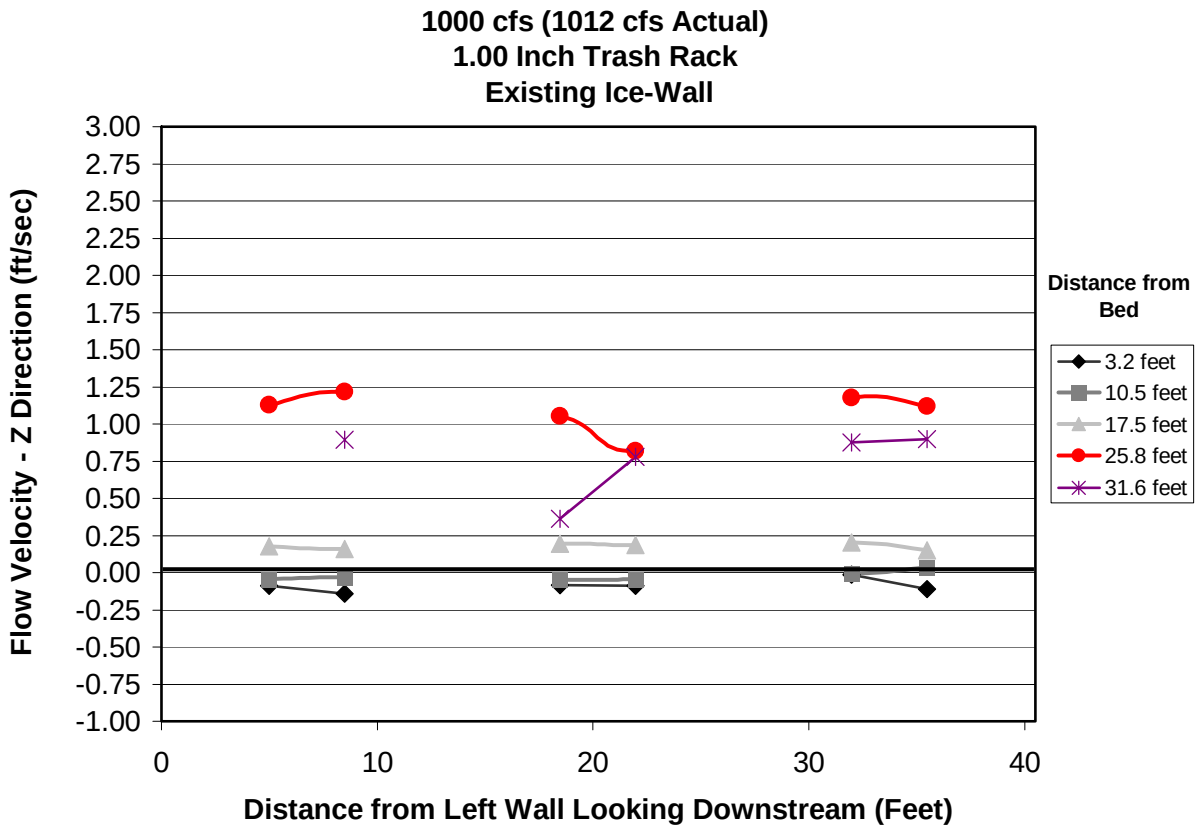

Figure C.9. The z-component of the velocity measured at 30 locations inside the bay areas, 2.9 ft away from a trash rack with 1.0-inch openings at its current location, under the 1000 cfs flow condition. The actual measured flow was 1012 cfs.

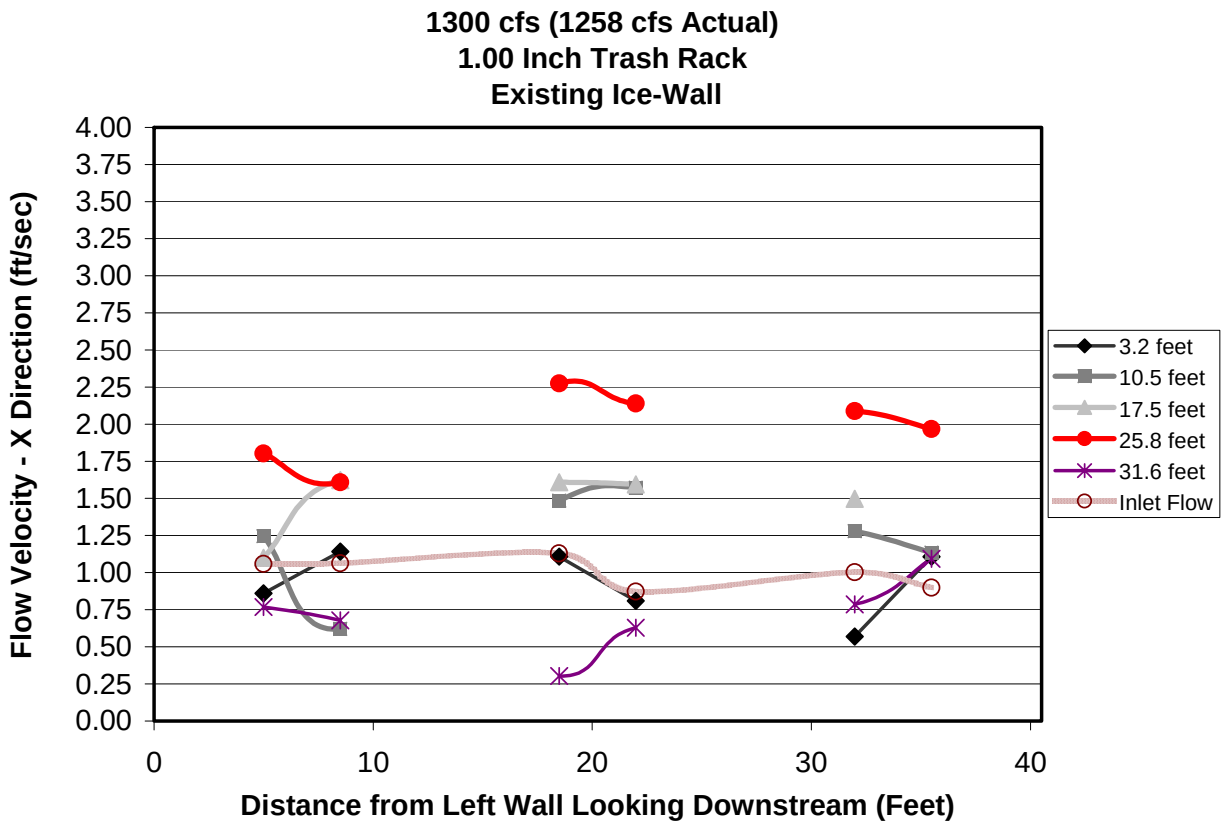

Figure C.10. The x-component of the velocity measured at 30 locations inside the bay areas, 2.9 ft away from a trash rack with 1.0-inch openings at its current location, under the 1300 cfs flow condition. The actual measured flow was 1258 cfs.

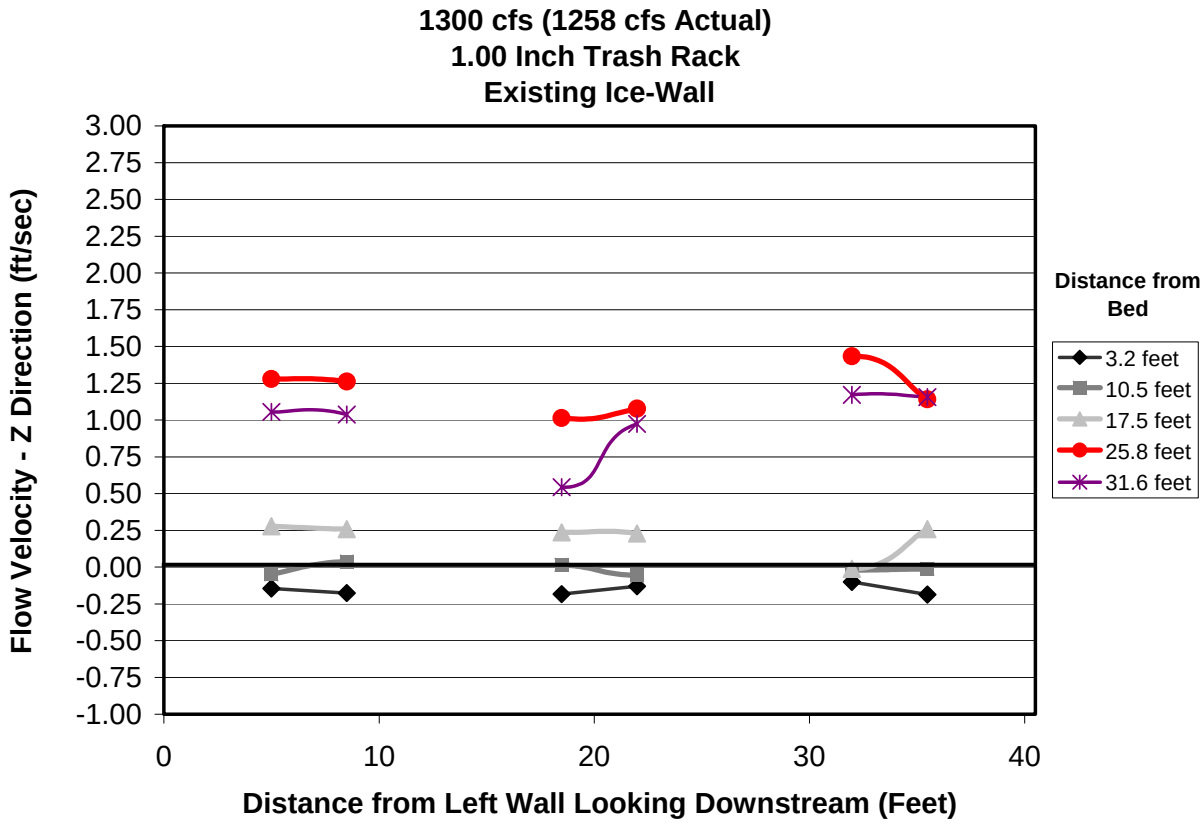

Figure C.11. The z-component of the velocity measured at 30 locations inside the bay areas, 2.9 ft away from a trash rack with 1.0-inch openings at its current location, under the 1300 cfs flow condition. The actual measured flow was 1258 cfs.

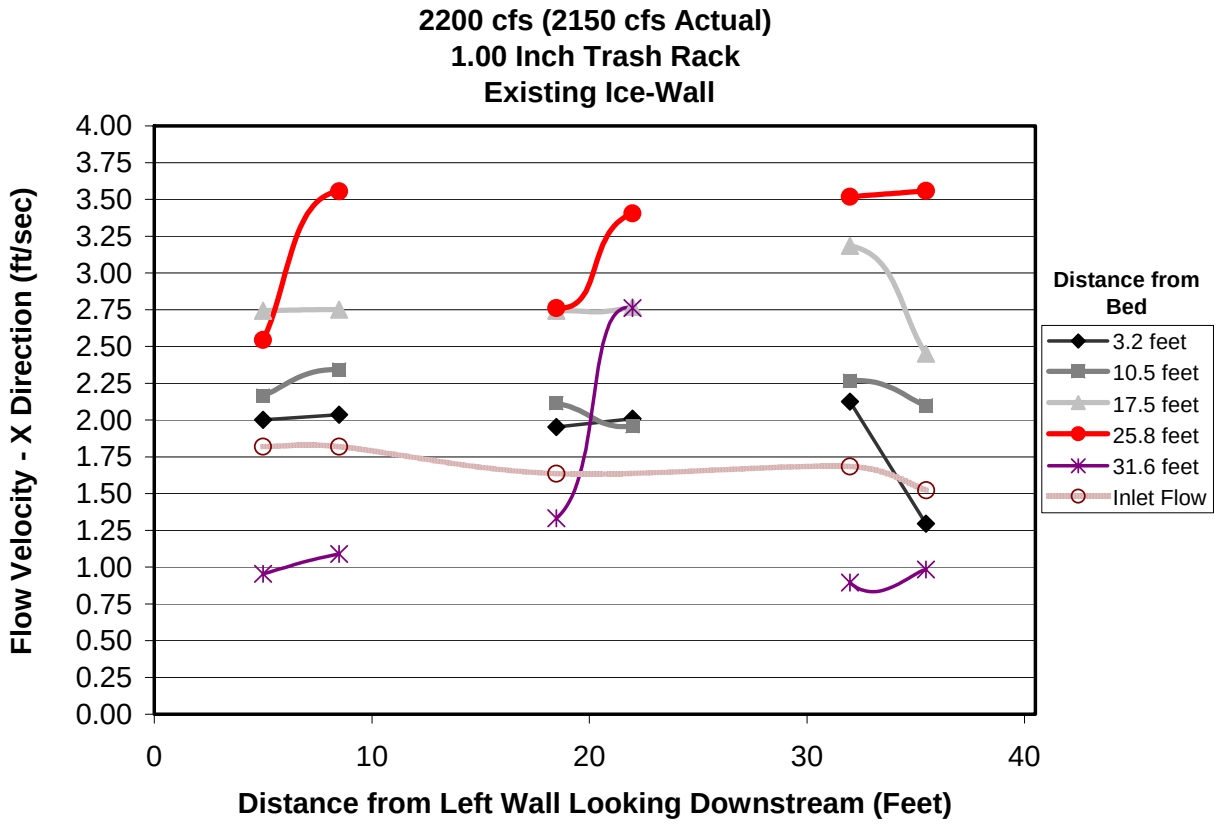

Figure C.12. The x-component of the velocity measured at 30 locations inside the bay areas, 2.9 ft away from a trash rack with 1.0-inch openings at its current location, under the 2200 cfs flow condition. The actual measured flow was 2150 cfs.

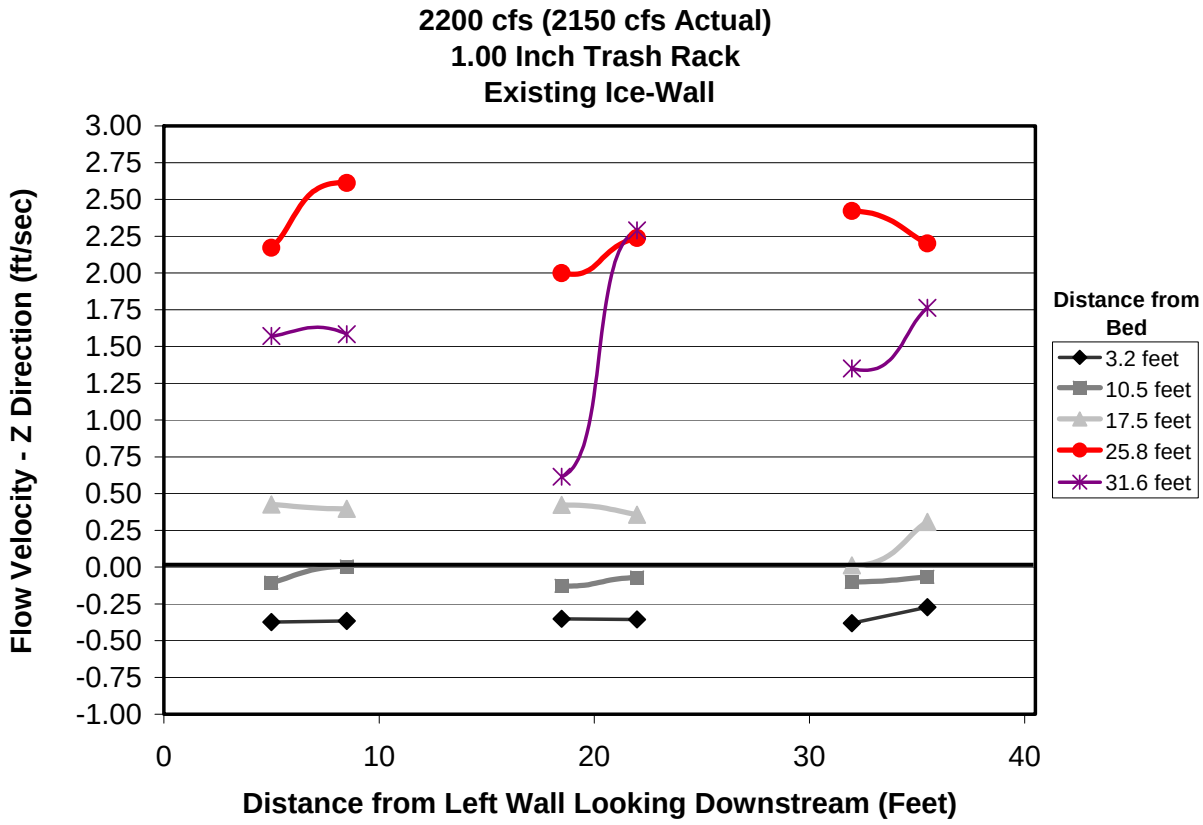

Figure C.13. The z-component of the velocity measured at 30 locations inside the bay areas, 2.9 ft away from a trash rack with 1.0-inch openings at its current location, under the 2200 cfs flow condition. The actual measured flow was 2150 cfs.

C.3. Test Series # 3: Ice-Wall with 3-ft Submergence and Trash Rack with 1.75-inch Openings

In the third test series, the submerged portion of the ice-wall was reduced to three feet under normal water level conditions, and the trash rack clear opening was 1.75 inches. The tests were conducted under four flow conditions: (1) 1000 cfs, (2) 1300 cfs, (4) 1600 cfs, and (4) 2200 cfs. Velocity components were measured at the same locations measured in the previous tests.

Under the 1000 cfs flow condition, the average measured x- and z-components of velocities were 0.99 fps and 0.01 fps, respectively, while the measured x-components of velocities were less than 1.4 fps (Figure C.14) and the measured z-components did not exceed 0.26 fps (Figure C.15).

Under the 1300 cfs flow condition, the average measured x- and z-components of velocities were 1.13 fps and 0.03, respectively, while the measured x-components of velocities did not exceed 1.8 fps (Figure C.16) and the measured z-components did not exceed 0.4 fps (Figure C.17).

Under the 1600 cfs flow condition, the average measured x- and z-components of velocities were 1.37 fps and 0.01, respectively, while the measured x-components of velocities did not exceed 2.6 fps (Figure C.18) and the measured z-components did not exceed 0.5 fps (Figure C.19)

Under the 2200 cfs flow condition, the average measured x- and z-components of velocities were 1.92 fps, 0.07 fps, respectively, while the x-components of velocities did not exceed 2.8 fps (Figure C.20) and the z-components did not exceed 0.7 fps (Figure C.21).

The maximum measured velocity occurred near the surface. The maximum velocity typically occurs near the lower end of the ice-wall, however, with a 3-ft ice-wall at about 2.9 feet away from the trash rack, the flow is redistributed and the maximum velocity may not be at the elevation of the lower end of the ice-wall.

In comparison to the first two test series, the velocities were more uniformly distributed across each depth due to a smaller confined space.

The qualitative analysis of the dye study indicated the presence of weak eddies between the ice-wall and the trash rack. Under all four flow conditions, the dye did not stay between the ice-wall and the trash rack long after the injection of the dye was stopped.

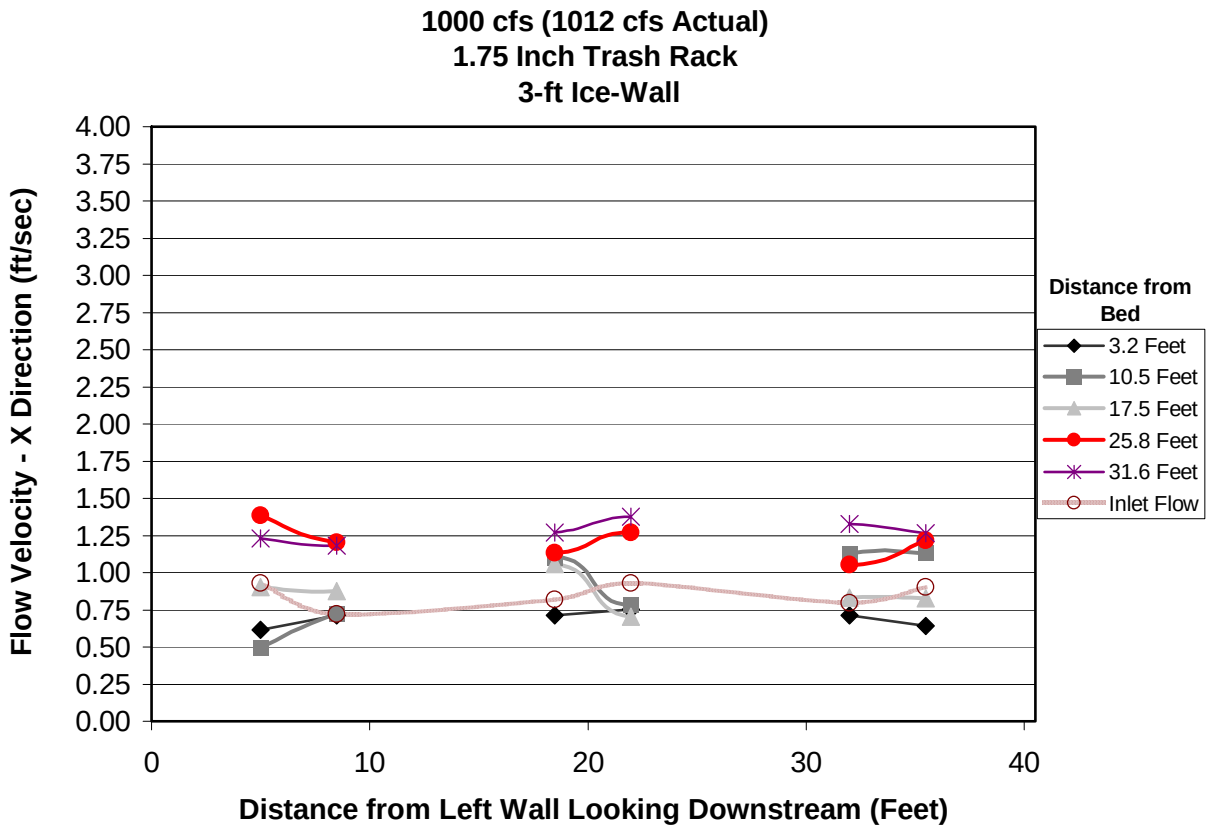

Figure C.14. The x-component of the velocity measured at 30 locations inside the bay areas, 2.9 ft away from a trash rack with 1.75-inch openings at its current location, under the 1000 cfs flow condition. The actual measured flow was 1012 cfs. The ice-wall was submerged 3-ft under normal water level conditions.

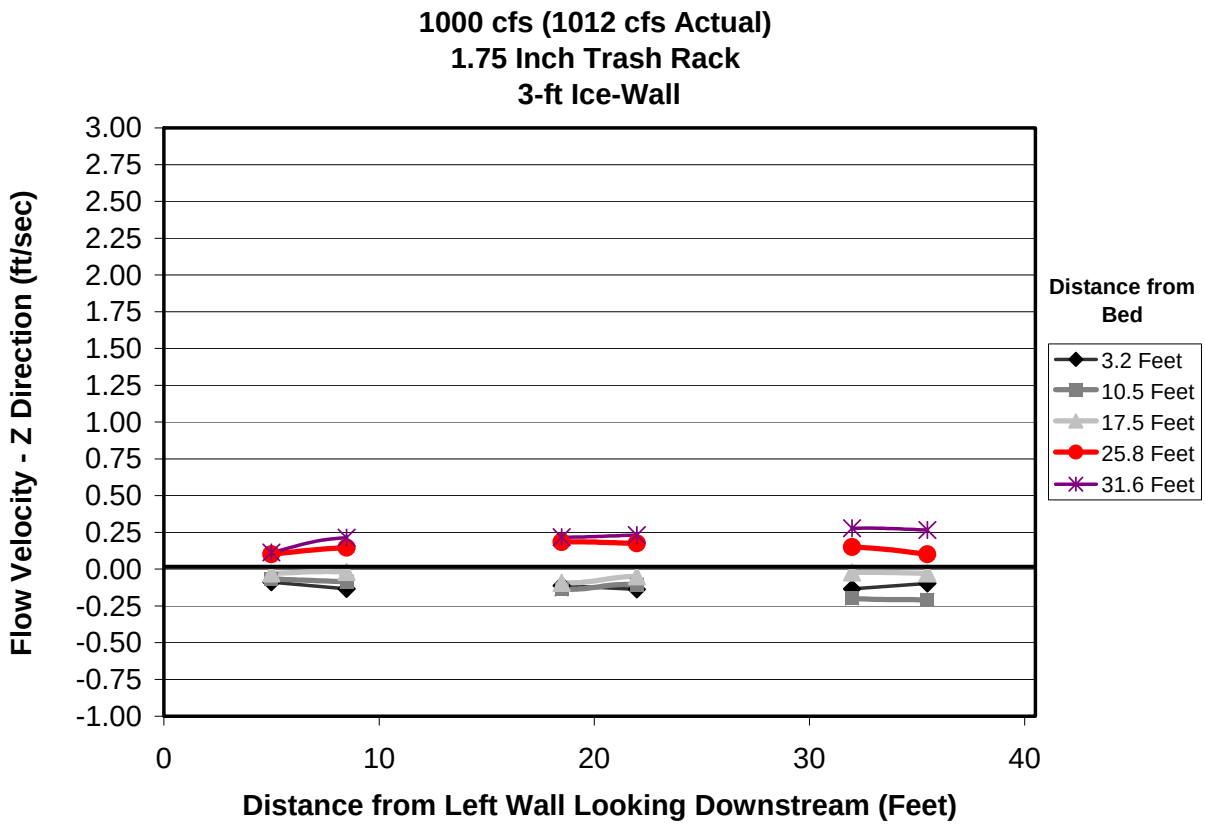

Figure C.15. The z-component of the velocity measured at 30 locations inside the bay areas, 2.9 ft away from a trash rack with 1.75-inch openings at its current location, under the 1000 cfs flow condition. The actual measured flow was 1012 cfs. The ice-wall was submerged 3-ft under normal water level conditions.

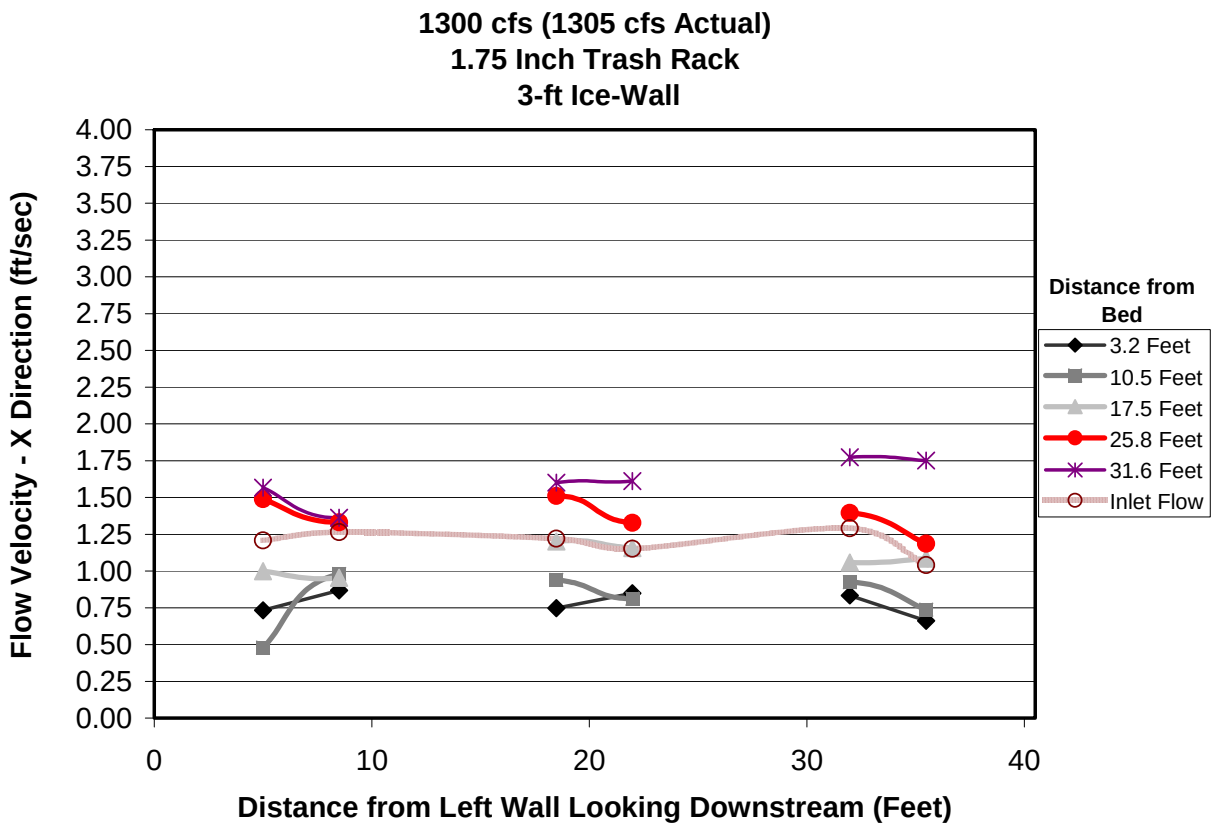

Figure C.16. The x-component of the velocity measured at 30 locations inside the bay areas, 2.9 ft away from a trash rack with 1.75-inch openings at its current location, under the 1300 cfs flow condition. The actual measured flow was 1305 cfs. The ice-wall was submerged 3-ft under normal water level conditions.

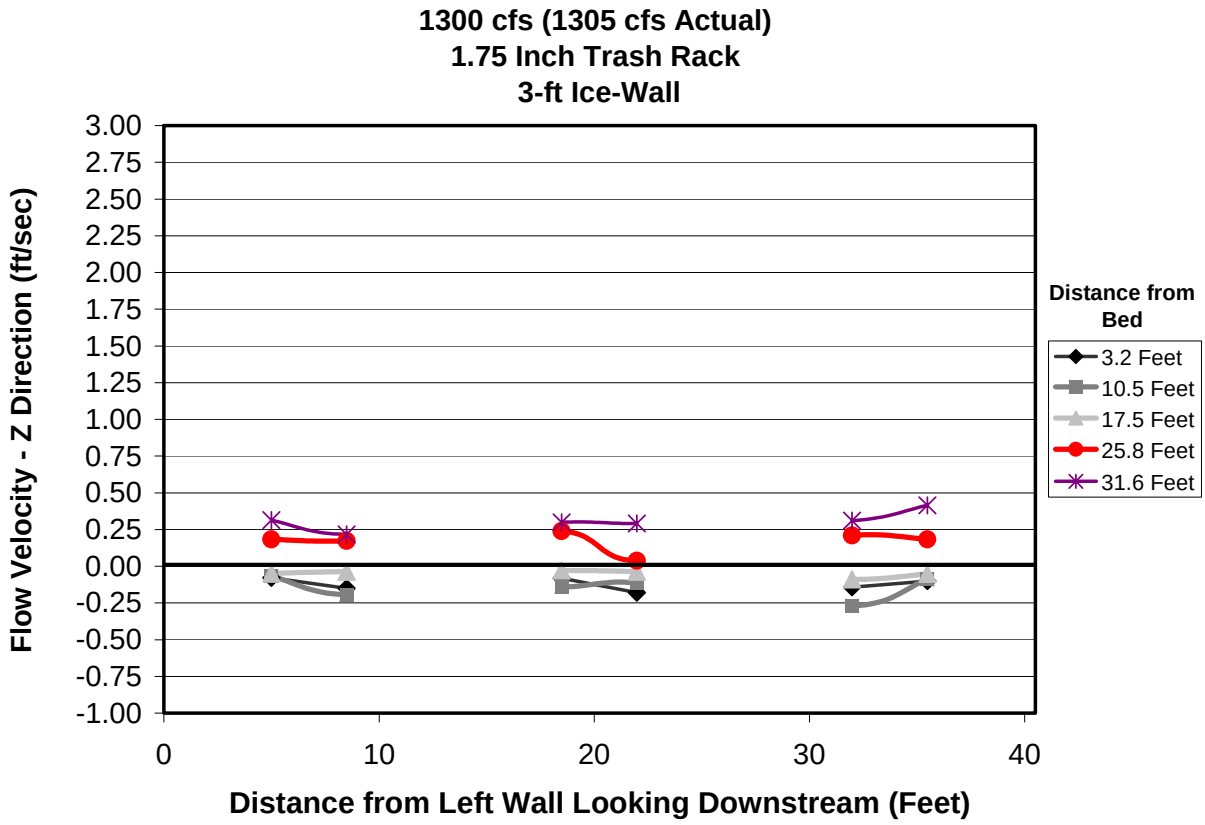

Figure C.17. The z-component of the velocity measured at 30 locations inside the bay areas, 2.9 ft away from a trash rack with 1.75-inch openings at its current location, under the 1300 cfs flow condition. The actual measured flow was 1305 cfs. The ice-wall was submerged 3-ft under normal water level conditions.

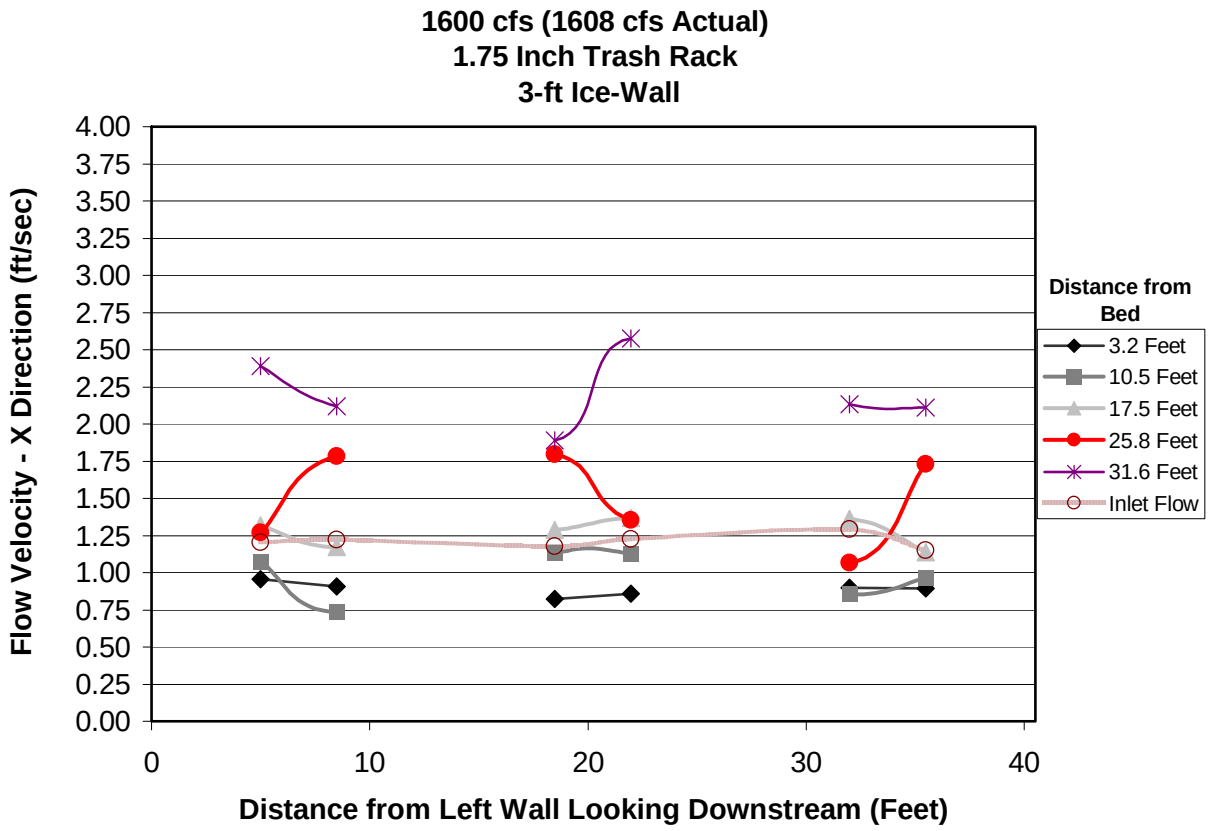

Figure C.18. The x-component of the velocity measured at 30 locations inside the bay areas, 2.9 ft away from a trash rack with 1.75-inch openings at its current location, under the 1600 cfs flow condition. The actual measured flow was 1608 cfs. The ice-wall was submerged 3-ft under normal water level conditions.

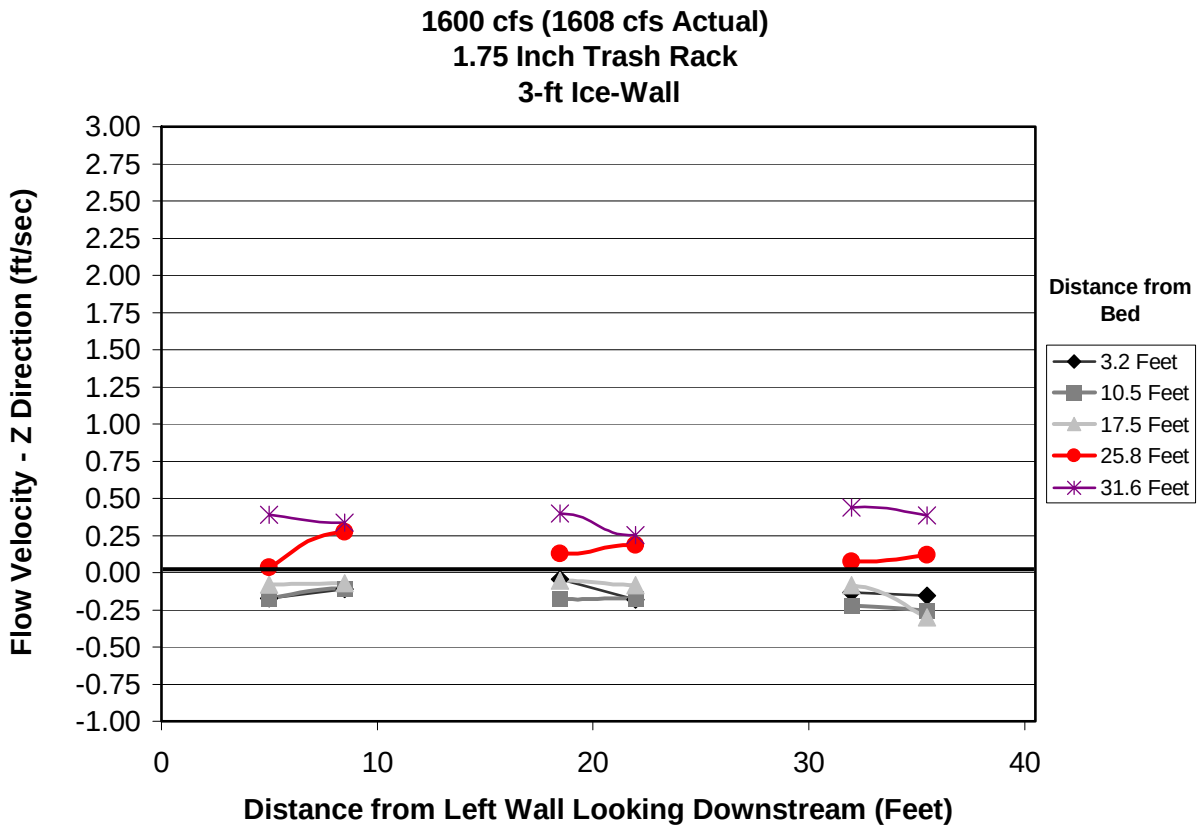

Figure C.19. The z-component of the velocity measured at 30 locations inside the bay areas, 2.9 ft away from a trash rack with 1.75-inch openings at its current location, under the 1600 cfs flow condition. The actual measured flow was 1608 cfs. The ice-wall was submerged 3-ft under normal water level conditions.

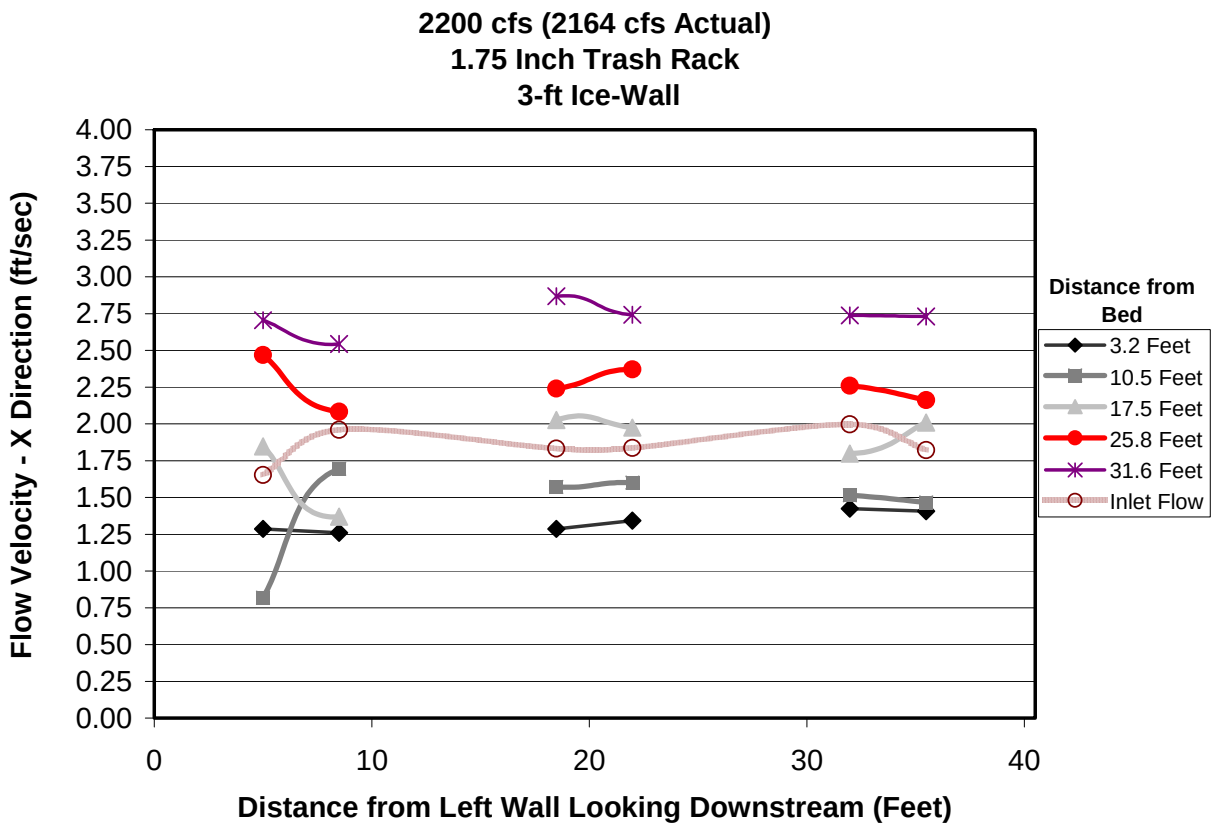

Figure C.20. The x-component of the velocity measured at 30 locations inside the bay areas, 2.9 ft away from a trash rack with 1.75-inch openings at its current location, under the 2200 cfs flow condition. The actual measured flow was 2164 cfs. The ice-wall was submerged 3-ft under normal water level conditions.

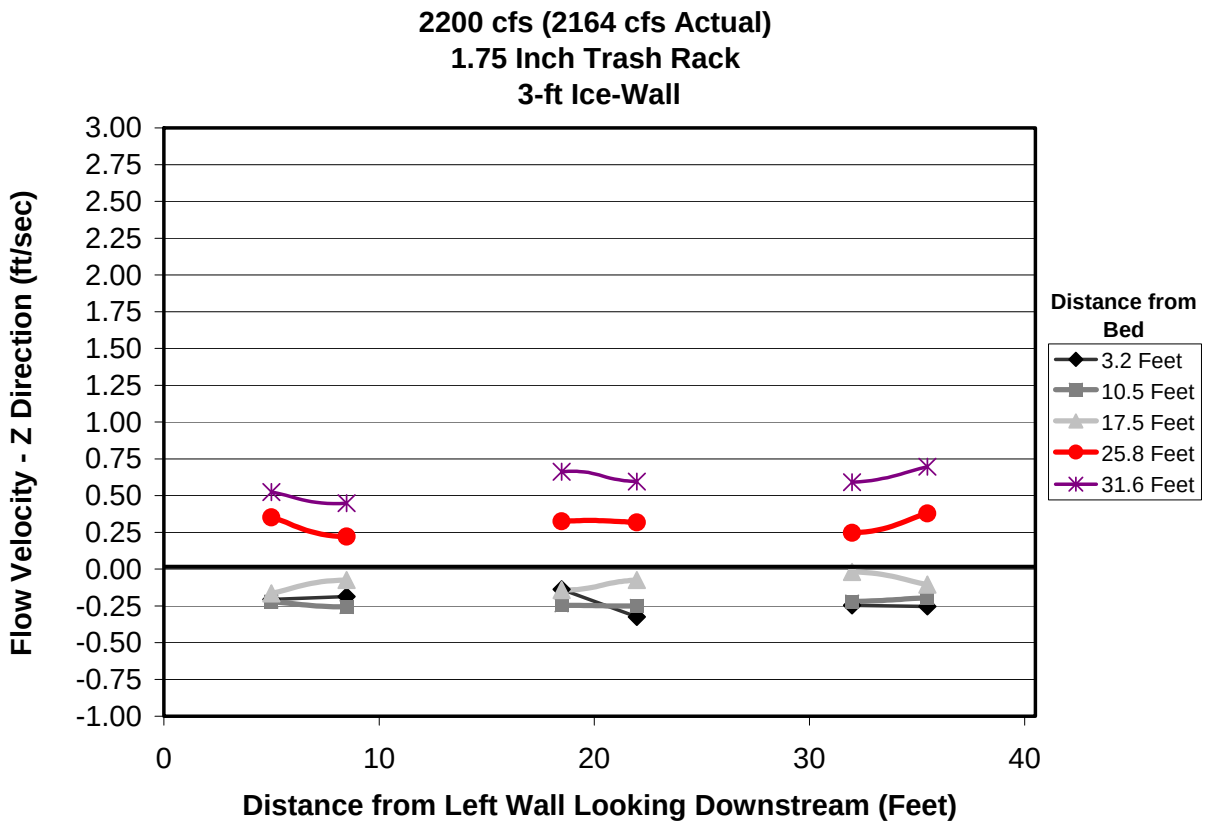

Figure C.21. The z-component of the velocity measured at 30 locations inside the bay areas, 2.9 ft away from a trash rack with 1.75-inch openings at its current location, under the 2200 cfs flow condition. The actual measured flow was 2164 cfs. The ice-wall was submerged 3-ft under normal water level conditions.

C.4. Test Series # 4: Ice-Wall with 3-ft Submergence and Trash Rack with 1.0-inch Openings

In the forth test series, the submerged portion of the ice-wall was reduced to under normal water level conditions, and the trash rack clear opening was 1.0 inch. The tests were conducted under the same flow conditions as in test series # 3 and velocity components were measured at the same locations.

Under the 1000 cfs flow condition, the average measured x- and z-components of velocities were 0.92 fps and 0.01 fps, respectively, while the measured x-components of velocities were less than 1.3 fps (Figure C.22) and the measured z-components did not exceed 0.3 fps (Figure C.23).

Under the 1300 cfs flow condition, the average measured x- and z-components of velocities were 1.12 fps and zero, respectively, while the measured x-components of velocities did not exceed 1.7 fps (Figure C.24) and the measured z-components did not exceed 0.3 fps (Figure C.25).

Under the 1600 cfs flow condition, the average measured x- and z-components of velocities were 1.39 fps and 0.03 fps, respectively, while the measured x-components of velocities did not exceed 2.1 fps (Figure C.26) and the measured z-components did not exceed 0.6 fps (Figure C.27).

Under the 2200 cfs flow condition, the average measured x- and z-components of velocities were 1.87 fps and 0.04 fps, respectively, while the x-components of velocities did not exceed 2.7 fps (Figure C.28) and the z-components did not exceed 0.8 fps (Figure C.29).

In comparison to test series # 3 with the 1.75-inch trash rack opening, the variation in measured velocities of this test series was slightly smaller.

Since the confined space between the trash rack and the ice-wall was smaller, less variability was evident in velocity measurements. However, a weak increasing trend in velocities was observed as the measurement location moved from the left wall to the right wall when looking downstream. This trend is attributed to the presence of a Plexiglas panel on the right outside wall which is smoother than a painted wooden wall in the model. Thus, the shear stress is smaller and allows more flow through the right bay.

The qualitative analysis of the dye study indicated the presence of weak eddies between the ice-wall and the trash rack. Under all four flow conditions, the dye did not stay between the ice-wall and the trash rack long after the injection of the dye was stopped.

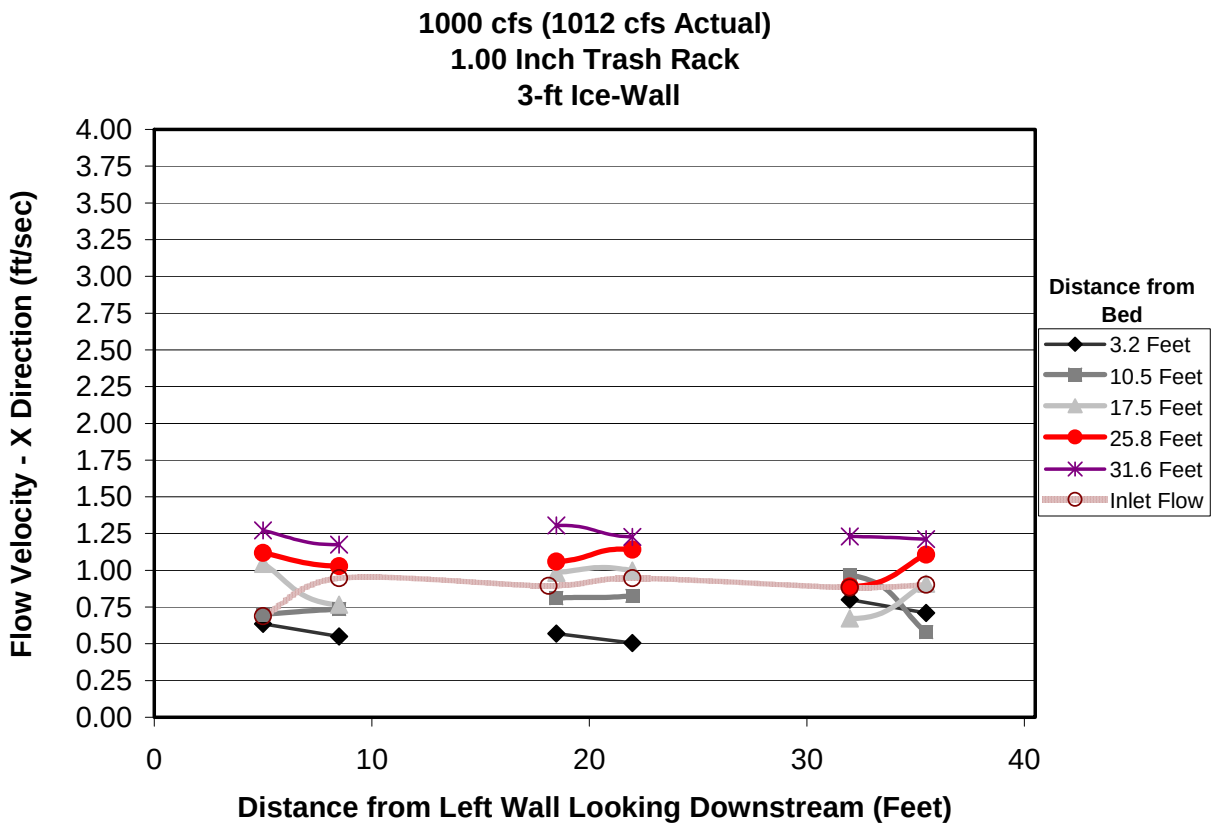

Figure C.22. The x-component of the velocity measured at 30 locations inside the bay areas, 2.9 ft away from a trash rack with 1.0-inch openings at its current location, under the 1000 cfs flow condition. The actual measured flow was 1012 cfs. The ice-wall was submerged 3-ft under normal water level conditions.

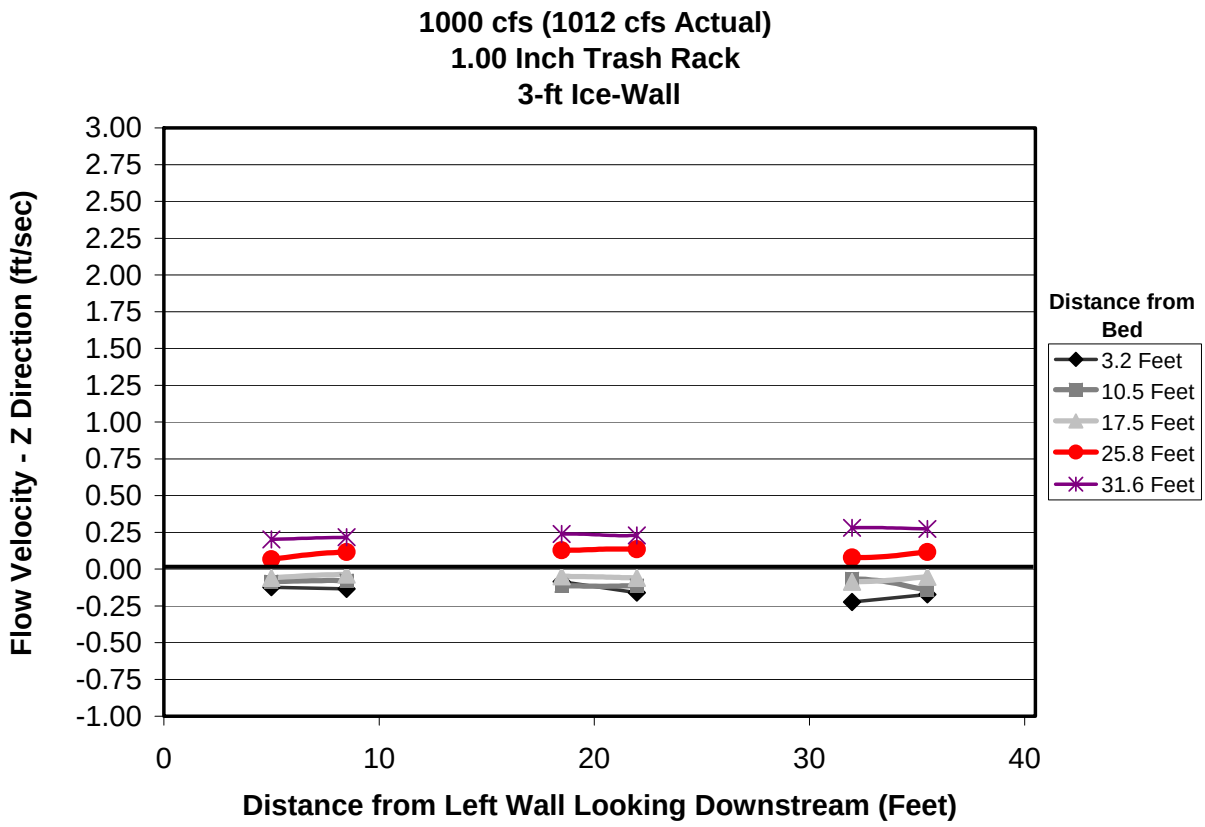

Figure C.23. The z-component of the velocity measured at 30 locations inside the bay areas, 2.9 ft away from a trash rack with 1.0-inch openings at its current location, under the 1000 cfs flow condition. The actual measured flow was 1012 cfs. The ice-wall was submerged 3-ft under normal water level conditions.

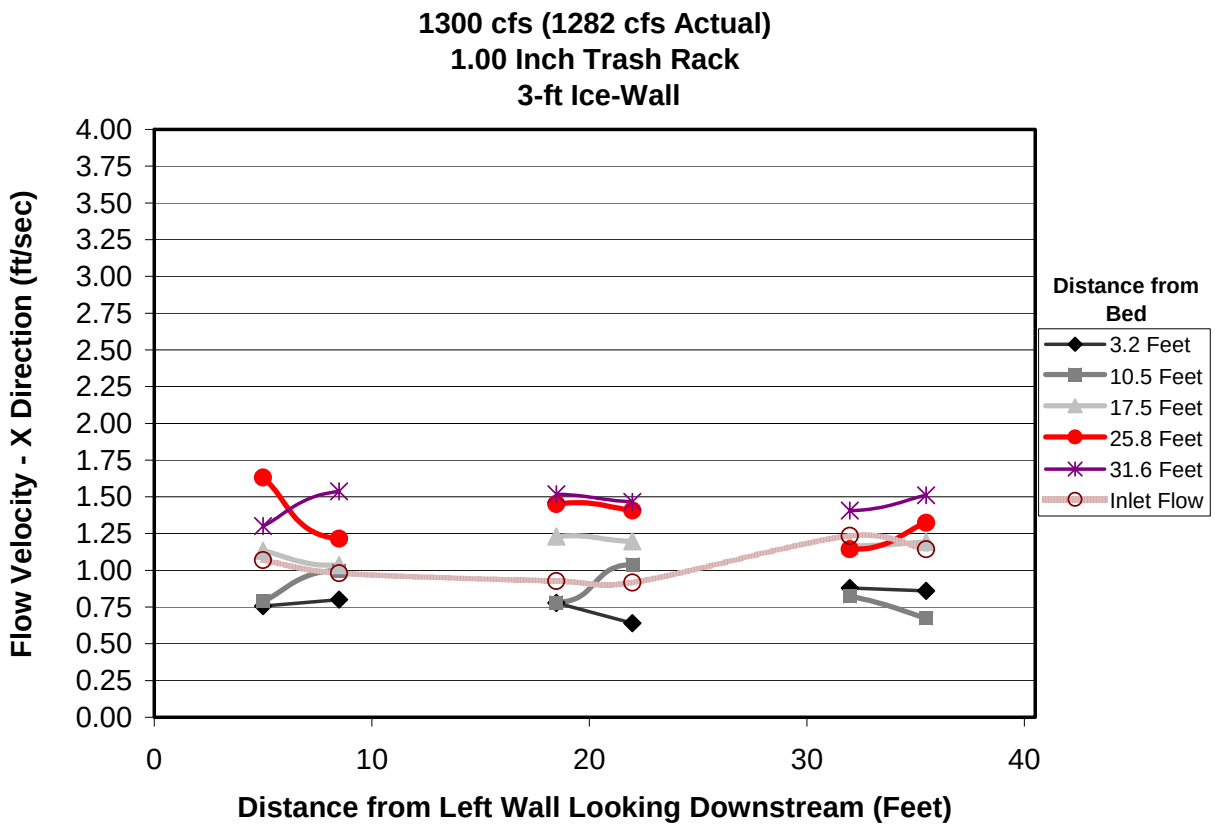

Figure C.24. The x-component of the velocity measured at 30 locations inside the bay areas, 2.9 ft away from a trash rack with 1.0-inch openings at its current location, under the 1300 cfs flow condition. The actual measured flow was 1282 cfs. The ice-wall was submerged 3-ft under normal water level conditions.

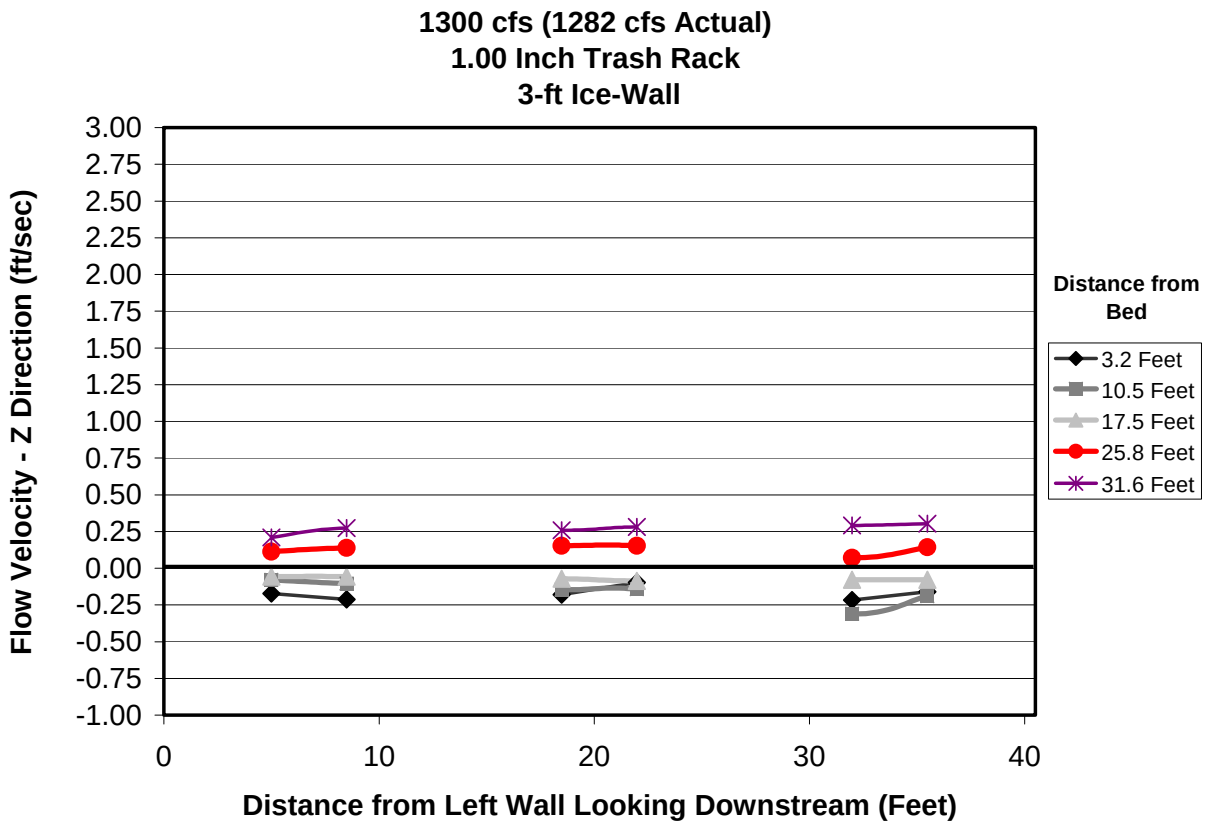

Figure C.25. The z-component of the velocity measured at 30 locations inside the bay areas, 2.9 ft away from a trash rack with 1.0-inch openings at its current location, under the 1300 cfs flow condition. The actual measured flow was 1282 cfs. The ice-wall was submerged 3-ft under normal water level conditions.

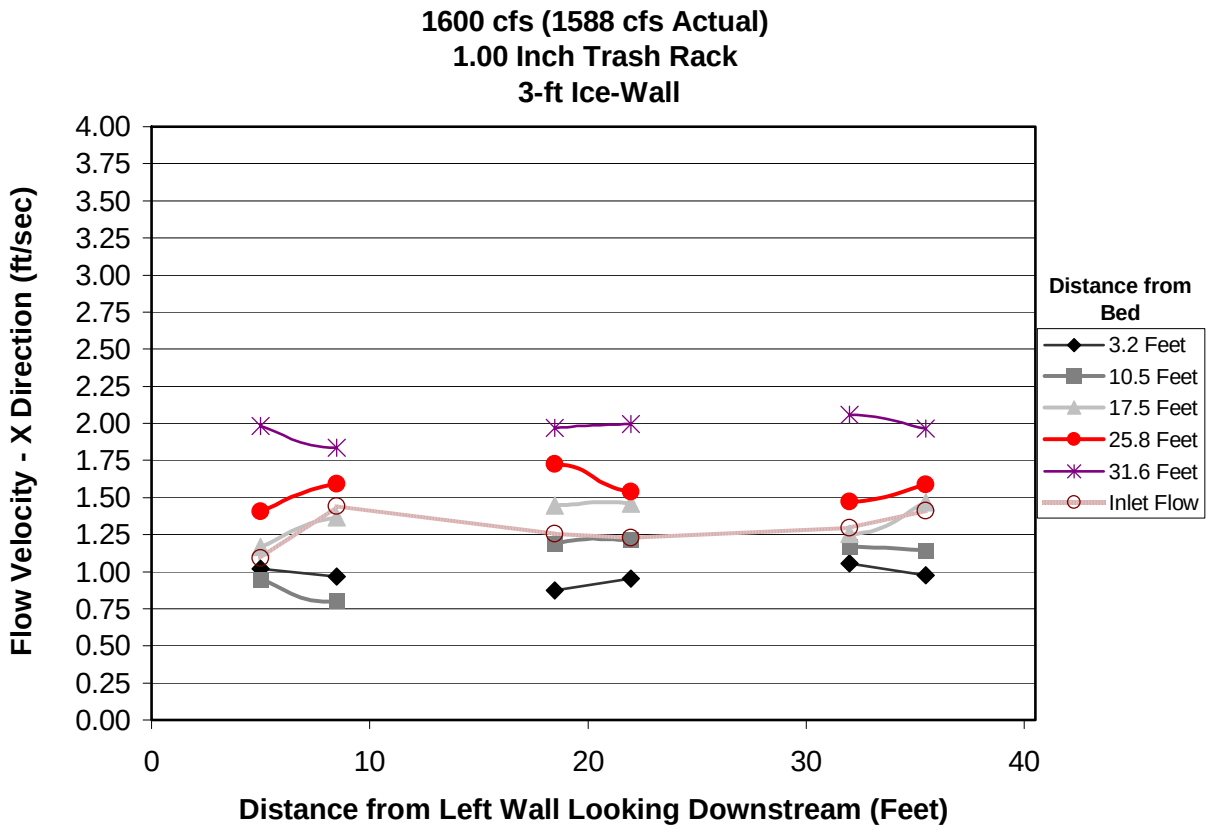

Figure C.26. The x-component of the velocity measured at 30 locations inside the bay areas, 2.9 ft away from a trash rack with 1.0-inch openings at its current location, under the 1600 cfs flow condition. The actual measured flow was 1588 cfs. The ice-wall was submerged 3-ft under normal water level conditions.

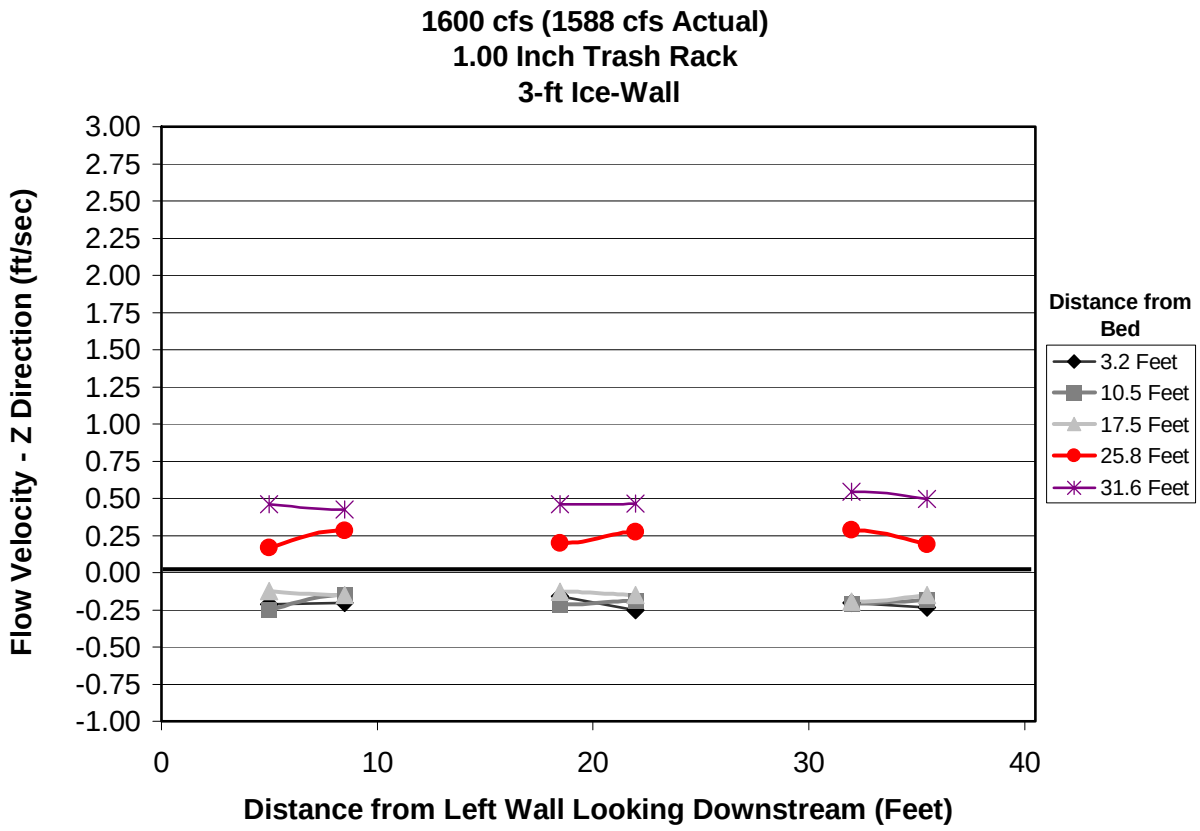

Figure C.27. The z-component of the velocity measured at 30 locations inside the bay areas, 2.9 ft away from a trash rack with 1.0-inch openings at its current location, under the 1600 cfs flow condition. The actual measured flow was 1588 cfs. The ice-wall was submerged 3-ft under normal water level conditions.

Figure C.28. The x-component of the velocity measured at 30 locations inside the bay areas, 2.9 ft away from a trash rack with 1.0-inch openings at its current location, under the 2200 cfs flow condition. The actual measured flow was 2156 cfs. The ice-wall was submerged 3-ft under normal water level conditions.

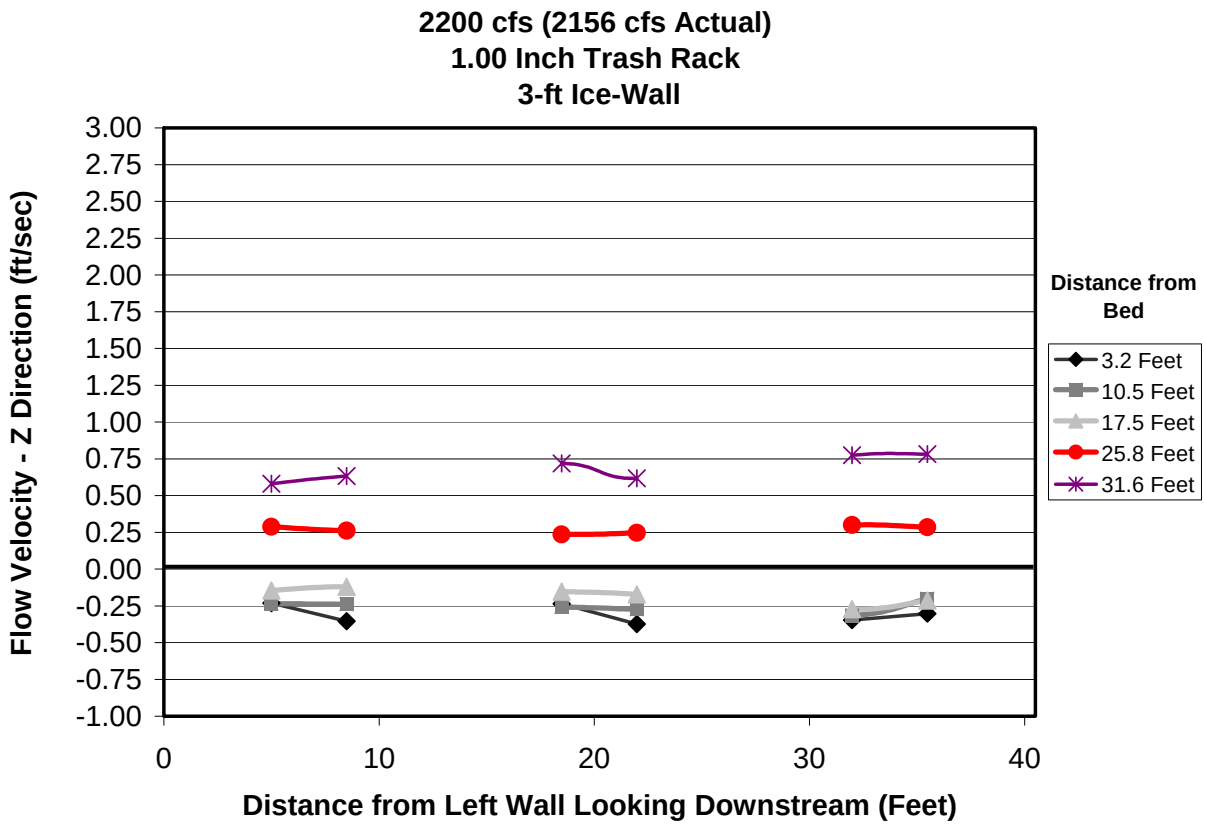

Figure C.29. The z-component of the velocity measured at 30 locations inside the bay areas, 2.9 ft away from a trash rack with 1.0-inch openings at its current location, under the 2200 cfs flow condition. The actual measured flow was 2156 cfs. The ice-wall was submerged 3-ft under normal water level conditions.

Appendix D: Intermediate Test Series

In the first two test series, the presence of large eddies between the ice-wall and the trash rack and velocities above 2 fps at the lower end of the ice-wall suggested that fish movement might be significantly affected by localized flow patterns. Therefore, it was decided to study potential modifications of the ice-wall.

It was clear that by decreasing the submergence of the ice-wall, the cross-sectional area of the approach flow would increase and thus the flow velocities at the lower end of the ice-wall would decrease. Since the model ice-wall was adjustable, a series of 12 tests were conducted under three ice-wall submergences (3-ft, 4-ft and 5-ft), two trash-rack openings, and two flow conditions: 1300 cfs and 2200 cfs. In the first two test series, the velocities at the lower end of the ice-wall under the 1000 cfs flow condition was less than 2 fps, therefore, the 1000 cfs flow condition did not seem to introduce any adverse condition for the fish species which would enter the region between the ice-wall and the trash rack.

For each test of this series, the velocity components were only measured at the lower end of the ice-wall in the middle bay. Since the velocities were measured at 10 locations across that depth, the average, maximum and minimum values of the x- and z-component of velocities were summarized in Table D.1. In addition, the magnitude of the resultant velocity was estimated using the three components of velocity. Furthermore, the flow patterns of all 12 tests were recorded.

The results of the tests show that under the 1300 cfs flow condition, the velocities near the lower end of the ice-wall do not reach 2 fps. The maximum recorded velocity was 1.79 fps. Under the 2200 cfs flow condition, average z-components varied from 0.2 fps (1-inch trash rack opening and 3-ft ice-wall) to 0.64 fps (1.75-inch trash rack opening and 5 ft ice-wall). The average x-components, however, exceeded 2 fps for all conditions but varied from 2.27 fps to 2.75 fps.

After reviewing the video clips of all 12 tests and the results of Table D.1, it was decided to conduct two more test series on an ice-wall with 3-ft submergence. The results of the test series are given in Appendix C.

Table D.1. Summary of the velocity measurements at the elevation of the lower end of the modified ice-wall and 2.9 feet away from the trash rack

Resultant Velocity (ft/sec)						
Ice-wall in water	**3 ft**		**4 ft**		**5 ft**	
Screen Size	**1 3/4"**	**1"**	**1 3/4"**	**1"**	**1 3/4"**	**1"**
Flow rates	**Velocity measured in middle bay at the height of the ice-wall**					
2200 cfs min	1.79	1.96	2.29	1.34	2.67	2.59
2200 cfs max	2.7	2.78	2.95	2.79	3.02	2.66
2200 cfs average	2.39	2.29	2.59	2.4	2.82	2.63
1300 cfs min	1.34	0.89	1.03	1.41	1.32	1.29
1300 cfs max	1.62	1.39	1.8	1.55	1.79	1.61
1300 cfs average	1.53	1.29	1.51	1.46	1.66	1.55
X-Component of Velocity (ft/sec)						
Ice-wall in water	**3 ft**		**4 ft**		**5 ft**	
Screen Size	**1 3/4"**	**1"**	**1 3/4"**	**1"**	**1 3/4"**	**1"**
Flow rates	**Velocity measured in middle bay at the height of the ice-wall**					
2200 cfs min	1.69	1.93	2.22	1.13	2.59	2.54
2200 cfs max	2.69	2.78	2.92	2.77	2.94	2.61
2200 cfs average	2.34	2.27	2.53	2.35	2.75	2.58
1300 cfs min	1.31	0.89	0.99	1.39	1.17	1.26
1300 cfs max	1.55	1.38	1.79	1.54	1.75	1.57
1300 cfs average	1.50	1.28	1.47	1.44	1.60	1.52
Z-Component of Velocity (ft/sec)						
Ice-wall in water	**3 ft**		**4 ft**		**5 ft**	
Screen Size	**1 3/4"**	**1"**	**1 3/4"**	**1"**	**1 3/4"**	**1"**
Flow rates	**Velocity measured in middle bay at the height of the ice-wall**					
2200 cfs min	0.18	0.09	0.15	0.18	0.63	0.51
2200 cfs max	0.43	0.27	0.56	0.41	0.66	0.53
2200 cfs average	0.30	0.20	0.43	0.36	0.64	0.52
1300 cfs min	0.10	0.05	0.19	0.09	0.25	0.23
1300 cfs max	0.25	0.18	0.31	0.25	0.40	0.34
1300 cfs average	0.22	0.16	0.27	0.22	0.32	0.32